JOURNAL OF PETROLOGY | VOLUME 39 | NUMBER 5 | PAGES 859–880 | 1998

Geochemistry of Jurassic Oceanic Crust beneath Gran Canaria (Canary Islands): Implications for Crustal Recycling and Assimilation

KAJ HOERNLE*

DEPARTMENT OF VOLCANOLOGY AND PETROLOGY, GEOMAR, WISCHHOFSTR. 1–3, D24148 KIEL, GERMANY

RECEIVED MAY 2, 1997; REVISED TYPESCRIPT ACCEPTED JANUARY 9, 1998

Trace elements and Sr–Nd–Pb isotopes have been analyzed on sedimentary and igneous (metabasalt, metadiorite and metagabbro) samples from the Jurassic oceanic crust beneath Gran Canaria (Canary Islands). The igneous crust exhibits extreme heterogeneity in $^{87}Sr/^{86}Sr$ (0·7029–0·7052), $^{206}Pb/^{204}Pb$ (18·2–20·8) and $^{208}Pb/^{204}Pb$ (38·1–41·3). Leaching experiments indicate that seawater alteration has elevated the $^{87}Sr/^{86}Sr$ ratio but has not appreciably affected $^{143}Nd/^{144}Nd$ (0·51295–0·51306). An Sm–Nd isochron gives an age of 178 ± 17 Ma, which agrees with the age predicted from paleomagnetic data. Hydrothermal alteration near the ridge axis has increased $^{207}Pb/^{204}Pb$ (15·59–15·73), $^{208}Pb/^{204}Pb$ (as well as Δ7/4Pb and Δ8/4Pb), $^{238}U/^{204}Pb$ (μ) and Ce/Pb but has not appreciably changed $^{206}Pb/^{204}Pb$. The large range in $^{206}Pb/^{204}Pb$ and $^{208}Pb/^{204}Pb$ reflects radiogenic ingrowth with μ being as high as 107. Portions of the Jurassic ocean crust have trace element and isotope characteristics within the range found at St Helena, the Atlantic type locality for the HIMU (high μ) mantle end-member. Evaluation of the published isotopic data for Gran Canaria volcanic rocks indicates that the isotopic composition of these melts primarily represents the composition of their mantle sources rather than crustal assimilation.

KEY WORDS: *Canary Islands; oceanic crustal recycling; seafloor hydrothermal alteration–metamorphism; HIMU; crustal assimilation in ocean island basalt*

INTRODUCTION

Overwhelming evidence that the mantle is heterogeneous on both small (mm) and large (global) scales has come from isotopic studies of ocean island basalts (OIB), fresh mid-ocean ridge basalt (MORB) glasses, mantle xenoliths and ultramafic massifs (e.g. Zindler & Hart, 1986). Recycling of oceanic crust through subduction zones is generally accepted as one of the major processes, if not the major process, causing heterogeneity within the mantle (e.g. Chase, 1981; Hofmann & White, 1982). Studies of Pb isotopes in OIB and MORB have been used to constrain the time necessary to recycle oceanic crust through subduction zones and have come up with widely differing estimates ranging from 300 to 2000 Ma (e.g. Sun, 1980; Silver *et al.*, 1988; Hanan & Graham, 1996; Thirlwall, 1997). Estimates of recycling ages are critically dependent on the effects of hydrothermal alteration near the ridge axis and the subduction process on the Pb isotope systematics of ocean crust.

Ocean island basalts have long been considered to be one of the major means for evaluating mantle heterogeneity, based on the belief that ocean crust, in contrast to continental crust, does not significantly contaminate ascending plume magmas. Indeed, several factors indicate that ocean crust is less likely to contaminate plume-derived magmas than continental crust. These factors include the smaller thickness, higher density and lower abundance of most incompatible elements in oceanic crust. In addition, oceanic crust is more similar in isotopic composition to mantle melts than to typical continental

*Telephone: 49-431-600-2642. Fax: 49-431-600-2964 or 2978. e-mail: khoernle@geomar.de

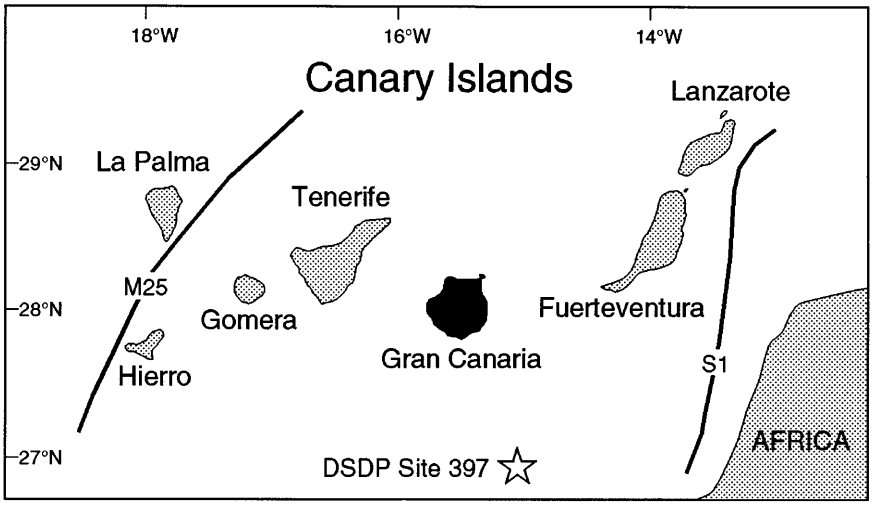

Fig. 1. Map of Canary Islands located in the eastern North Atlantic Ocean off the coast of northwest Africa. Approximate locations of the M25 (156 Ma) and S1 (175 Ma) paleomagnetic anomalies are also shown (Roeser, 1982; Klitgord & Schouten, 1986; Roest *et al.*, 1992).

crust. Several recent studies, using thorium, oxygen and osmium isotope systems, however, suggest that crustal contamination can affect the chemistry of ocean island magmas (e.g. Nicholson *et al.*, 1991; Marcantonio *et al.*, 1995; Widom & Shirey, 1996; Eiler *et al.*, 1996*a*, 1996*b*; Thirlwall *et al.*, 1997). To more fully evaluate the role of crustal contamination on ocean island magmas, it is necessary to improve our understanding of the range in composition of altered and aged oceanic crust.

In this study, an extensive trace element and Sr–Nd–Pb isotope data set is presented for the Jurassic oceanic crust beneath Gran Canaria. As the Canary Islands are located on some of the oldest oceanic crust, this crust serves as an end-member for evaluating the effects of (1) alteration processes, (2) radiogenic ingrowth and (3) contamination of plume-derived, ocean-island melts. Furthermore, because of the proximity of Gran Canaria to the African continental margin (Fig. 1) and its old age, Gran Canaria is situated on one of the thickest packages of sediments (~6 km) of all ocean islands, enhancing the possibility of sediment assimilation during magma ascent. Finally, volcanic and plutonic rocks from Gran Canaria have been extensively studied for trace element and Sr–Nd–Pb–O isotopic compositions (e.g. Sun, 1980; Schmincke, 1982; Crisp & Spera, 1987; Cousens *et al.*, 1990, 1993; Hoernle *et al.*, 1991; Hoernle & Schmincke, 1993*a*, 1993*b*; Freundt & Schmincke, 1995; Thirlwall *et al.*, 1997; Wiechert *et al.*, 1997). To date, evidence for crustal assimilation has only been noticed in the Miocene volcanic rocks (Freundt & Schmincke, 1995; Thirlwall *et al.*, 1997). Two major goals of this paper are (1) to constrain the age of ocean crust recycling and the origin of the HIMU component in OIB, and (2) to evaluate the role of crustal assimilation on the chemistry of OIB.

GENERAL GEOLOGY

The Canary Islands, located in the Atlantic Ocean off the coast of NW Africa (Fig. 1), sit on Jurassic ocean crust, some of the oldest *in situ* crust in the ocean basins. The age of the crust beneath the Canary Islands can be bracketed by the 175 Ma S1 magnetic anomaly between the easternmost Canary Islands and northwest Africa and the 156 Ma M25 magnetic anomaly between the westernmost islands of La Palma and Hierro (Roeser, 1982; Klitgord & Schouten, 1986; Roest *et al.*, 1992). Gran Canaria, the third easternmost island, lies on ocean crust in the Jurassic magnetic quiet zone between these two anomalies. The thickness of the oceanic crust to the north and northeast of Gran Canaria is ~10 km (Schmincke *et al.*, 1997; Ye *et al.*, 1998). Layer 1 consists of ~6 km of mid-Miocene to Jurassic sediments and possibly a Jurassic carbonate platform. Layer 2 (pillows and dikes or sills) is ~2 km thick, whereas crustal layer 3 (intrusives, primarily gabbros) has a thickness of ~2·5 km.

The 15 my subaerial volcanic history of Gran Canaria (Schmincke, 1982; Hoernle & Schmincke, 1993*a*, 1993*b*) can be divided into two major cycles of volcanic activity: (1) Miocene or shield cycle (~10–15 Ma) and (2) post-Miocene rejuvenated (post-erosional) cycle(s) (~0–5·5 Ma). The tholeiitic to alkalic shield basalts (~14–15 Ma) form the oldest and most voluminous subaerially exposed unit. At 14 Ma, a composite peralkaline rhyolite–basalt ignimbrite (P1) was erupted, resulting in caldera formation. Peralkaline rhyolites and trachytes, and rare alkali basalts and intermediate rocks, were erupted for the next ~1 my. Between ~10 and 13 Ma, volcanic rocks became more SiO_2 undersaturated, ranging from trachytes to phonolites, including rare basanites and

nephelinites. In summary, volcanic and plutonic rocks became more evolved and SiO_2 undersaturated with decreasing age during the Miocene cycle of volcanism. Eruption and magma production rates also generally decreased during the Miocene.

After an ~4·5 my hiatus in volcanism, the post-Miocene cycle began ~5·5 my ago with eruption of small volumes of highly undersaturated nephelinitic and basanitic lavas. As eruption rates and magma production rates increased with decreasing age, alkali basalt became dominant. A single interval of tholeiitic pahoehoe flows (representing several km^3 in volume) was erupted during this time interval. The peak of activity was reached ~4 my ago. Between 3·5 and 4·0 Ma, complete suites of alkali basalt to trachyte and basanite to phonolite were erupted, with more evolved compositions dominating. Although the degree of differentiation generally increases up-section, basalts and evolved volcanic rocks are intercalated throughout this time interval. Between 0 and 3·0 Ma, eruptives consisted primarily of basanite, nephelinite and melilite-bearing nephelinite.

SAMPLE DESCRIPTION

The carbonate and silicic sediment samples (layer 1) occur as xenoliths within late Pliocene and Quaternary mafic lava flows and come from Deep Sea Drilling Project (DSDP) Site 397, ~100 km southeast of Gran Canaria. The igneous crustal samples (layers 2 and 3) occur as cobbles within a Miocene (~14 Ma) fanglomerate exposed at the bottom of Barranco (Canyon) de Balos in the SE portion of Gran Canaria, and are interpreted to have been brought to the surface in phreatic eruptions (Schmincke *et al.*, 1998). These samples consist primarily of greenschist facies metabasalts, metadiorites and metagabbros, but also include some relatively fresh coarse-grained gabbros with 2 cm long plagioclase. Some metabasalt clasts appear to represent fragments of pillows or dikes, as is evident from their fine-grained margins.

Petrography, mineral chemistry, and major and trace element data from X-ray fluorescence (XRF) have been presented by Schmincke *et al.* (1998) and therefore are only briefly summarized here. Primary igneous minerals are calcic plagioclase, augitic clinopyroxene $\pm$ orthopyroxene and Fe–Ti oxides. The primary mineralogy has been modified to variable extents at upper greenschist facies conditions, as reflected by secondary actinolite or ferroactinolite, Fe–Mg chlorite, epidote, sphene, ilmenite $\pm$ hematite, Ab-rich plagioclase, muscovite, biotite and iron sulfide. Most fine-grained metabasalts (e.g. sample 303905) consist almost entirely of the greenschist facies phase assemblages; however, many of the coarser-grained samples contain igneous plagioclase and pyroxene with optically fresh cores (e.g. samples B914, B9112, 412938). Within sample B9117, the degree of hydrothermal alteration, as indicated by the abundance of secondary phases such as chlorite, Fe-actinolite and epidote, increases from B9117.1 (relatively fresh) to B9117.3 (the most altered). Igneous samples are mafic (7·4–10·8% MgO, 78–206 ppm Ni and 79–516 ppm Cr) and have tholeiitic compositions (48–53% SiO_2).

ANALYTICAL METHODS

Chips from the interior of samples (to minimize alteration after subaerial exposure) were ground to a flour in an agate mill. Plagioclase separates were prepared by picking under a binocular microscope and then rinsed with cold 3 N HNO_3. Trace elements on the samples were analyzed with a VG Plasmaquad PQ1 inductively coupled plasma-mass spectrometer at the Geological Institute, Christian Albrechts University in Kiel, using the method of Garbe-Schönberg (1993). The trace element data, replicate analyses and standards (except for house standards) run during the study are presented in Table 1.

The Sr, Nd and Pb isotopic compositions of whole-rock and plagioclase samples were determined by thermal-ionization mass spectrometry (TIMS) at the Universities of California in Santa Barbara (on a Finnigan MAT261 mass spectrometer) and Santa Cruz (on a VG Sector 54-30 mass spectrometer). Analytical procedures are the same as those outlined by Hoernle & Tilton (1991). A second split of powder for samples 303903, 303905 and 303906 (denoted by a.w.—acid washed) were boiled in a mixture of 50% 6 N HCl and 50% 8 N HNO_3 for 1 h. The residues were analyzed for their Sr and Nd isotopic composition. The measured $^{87}Sr/^{86}Sr$ ratio was normalized within-run to $^{86}Sr/^{88}Sr = 0{\cdot}1194$ and then to an $^{87}Sr/^{86}Sr$ value of 0·710235 for NBS987. The $^{143}Nd/^{144}Nd$ ratio was normalized within-run to $^{146}Nd/^{144}Nd = 0{\cdot}7219$ and then to a $^{143}Nd/^{144}Nd$ value of 0·51185 for the La Jolla standard. $^{143}Nd/^{144}Nd$ ratios were measured in dynamic mode. The Pb isotope data are corrected for mass fractionation using a factor of 0·11% per atomic mass unit for the Santa Cruz data (samples 303903, 303905 and 303906) and 0·125% for the Santa Barbara data (all other samples).

TRACE ELEMENT AND ISOTOPE DATA

The trace element data for Jurassic ocean crust samples from Gran Canaria are presented in Table 1. Immobile incompatible elements, such as Th, Nb, Ta and the rare earth elements (REE), of igneous samples, show good correlations with each other (Fig. 2). Th and U also correlate well (Fig. 3). Incompatible element abundances

Table 1: Trace element concentrations (in ppm) from ICP-MS for samples from ocean crust layer 1 (sediments), layer 2 (pillow lavas, sheet flows and dikes) and layer 3 (gabbros) beneath Gran Canaria; also shown are means for analyses of standards BHVO-1 and BIR-2 and blanks, as well as 1σ standard deviations of BHVO-1

Sample:	917c	91249	303905	303906	B9117.1	B9117.2	B9117.3	303903	B913	B914	B914	B914	B9112	B9112	412938	B9114	BHV0-1	SD	BIR-2	Blank
Crustal layer:	1	1	2	2	2	2	2	3	3	3	3	3	3	3	3	3				
	Sediment xenolith	Sediment xenolith	Tholeiitic basalt	Tholeiitic basalt	Tholeiitic basalt	Tholeiitic basalt	Tholeiitic basalt	Tholeiitic gabbro	Tholeiitic gabbro	Tholeiitic gabbro	Plagioclase separate	Plagioclase separate	Tholeiitic gabbro	Tholeiitic gabbro	Tholeiitic gabbro	Tholeiitic gabbro		$n = 6$		
Li	14·5	11·8	7·68	13·0	0·02	0·02	0·57	0·61	19·6	0·950	2·15	0·24	0·88	1·03	1·54		5·25	0·06	3·32	0·000040
Sc	4·92	5·28	42·2	27·4	44·4	42·9	48·4	38·9	26·3	40·6	3·63	3·26	31·2	31·4	35·7	47·7	34·5	0·1	45·7	0·000130
Cu	65·1	24·9	47·6	72·6	15·7	14·9	16·7	46·8	82·3	40·9	6·85	6·73	40·0	39·7	54·1	58·9	150	3	131	0·000070
Zn	28·4	55·4	59·9	84·0	44·8	44·7	50·6	68·2	101	42·4	15·0	14·0	55·2	54·4	25·9	121	123	2	75·9	0·000070
Ga	6·17	5·78	12·7	15·5	15·7	15·3	15·6	13·3	13·5	12·6	19·0	19·0	12·0	12·2	10·0	14·4	23·4	0·6	16·0	0·000010
Rb	31·7	35·5	1·05	5·92	0·52	0·44	0·71	0·31	1·40	2·01	0·82	0·83	1·28	1·36	0·17	1·39	9·68	0·29	0·23	0·000020
Sr	113	92·9	158	123	129	121	129	60·2	36·4	91·2	162	161	72·9	74·0	69·4	96·5	422	14	117	0·000190
Y	8·57	8·95	25·7	22·7	23·1	22·4	23·1	22·0	16·2	8·80	0·36	0·421	14·4	14·4	5·30	12·8	24·6	2·4	16·5	0·000010
Zr	25·6	21·9	31·0	45·5	34·3	31·6	35·0	19·0	29·7	7·10	0·71	0·59	18·1	17·0	3·60	11·6	170	5	14·9	0·000010
Nb	6·50	5·16	4·71	11·7	10·7	10·4	9·94	3·48	9·08	0·51	0·10	0·09	3·59	3·64	0·21	1·26	18·1	0·9	0·56	0·000000
Ba	131	139	44·6	68·1	31·2	29·9	36·4	54·0	13·3	38·0	35·2	35·6	23·5	25·9	13·3	24·5	136	3	7·20	0·000240
La	14·0	15·1	3·72	10·5	6·69	6·43	8·12	2·60	6·84	0·85	1·09	1·08	2·63	2·55	0·39	1·16	15·8	0·3	0·63	0·000080
Ce	28·0	29·8	8·43	21·7	14·1	13·7	16·1	6·35	13·41	2·03	1·70	1·71	6·98	6·94	0·96	2·84	37·7	0·6	2·02	0·000020
Pr	3·23	3·40	1·29	2·77	1·95	1·94	2·04	0·98	1·72	0·30	0·19	0·19	0·85	0·84	0·15	0·46	5·31	0·16	0·40	0·000000
Nd	12·0	12·4	6·62	12·1	8·65	8·45	8·79	5·18	7·18	1·65	0·77	0·75	4·20	4·21	0·92	2·44	24·0	0·6	2·47	0·000020
Sm	2·49	2·68	2·29	3·08	2·41	2·43	2·50	1·90	1·95	0·68	0·17	0·15	1·37	1·42	0·41	0·93	5·99	0·22	1·16	0·000010
Eu	0·53	0·57	0·82	0·91	0·84	0·84	0·86	0·71	0·72	0·42	0·55	0·54	0·54	0·54	0·23	0·52	2·00	0·09	0·53	0·000010
Gd	2·26	2·56	3·18	3·49	2·92	2·99	3·01	2·70	2·33	0·95	0·16	0·17	1·90	1·79	0·59	1·36	6·11	0·14	1·86	0·000020
Tb	0·31	0·34	0·62	0·63	0·53	0·54	0·53	0·52	0·42	0·21	0·02	0·02	0·35	0·35	0·12	0·27	0·92	0·03	0·38	0·000010
Dy	1·61	1·70	4·30	3·89	3·55	3·59	3·58	3·63	2·77	1·41	0·12	0·14	2·40	2·39	0·86	1·92	5·15	0·23	2·61	0·000010
Ho	0·28	0·30	0·92	0·81	0·89	0·76	0·76	0·80	0·58	0·32	0·02	0·03	0·53	0·52	0·20	0·42	0·95	0·03	0·58	0·000010
Er	0·78	0·80	2·79	2·38	2·44	2·21	2·26	2·40	1·72	0·95	0·06	0·06	1·57	1·55	0·58	1·26	2·46	0·08	1·74	0·000010
Tm	0·11	0·11	0·40	0·34	0·46	0·32	0·32	0·34	0·25	0·14	0·01	0·01	0·23	0·22	0·08	0·19	0·33	0·01	0·25	0·000010
Yb	0·64	0·68	2·68	2·14	2·27	2·10	2·09	2·27	1·64	0·95	0·07	0·06	1·52	1·49	0·56	1·30	1·97	0·06	1·67	0·000020
Lu	0·09	0·10	0·40	0·31	0·34	0·30	0·31	0·33	0·25	0·14	0·01	0·01	0·22	0·22	0·09	0·19	0·27	0·01	0·25	0·000010
Hf	0·66	0·62	1·21	1·53	1·13	1·11	1·03	0·68	0·99	0·26	0·02	0·01	0·62	0·59	0·12	0·38	4·45	0·23	0·60	0·000020
Ta	0·53	0·43	0·28	0·70	0·59	0·56		0·19	0·53	0·04	0·04	0·04	0·22	0·21	0·01	0·07	1·10	0·06	0·04	0·000000
Pb	3·89	26·9	0·31	3·56	0·67	0·36	0·13	0·54	1·94	0·41	0·14	0·16	0·32	0·29	0·25	0·83	2·08	0·08	3·28	0·000020
Th	3·62	3·22	0·32	1·26	0·87	0·71	0·72	0·24	0·62	0·12	0·06	0·06	0·23	0·22	0·03	0·15	1·20	0·07	0·03	0·000000
U	0·52	0·55	0·07	0·33	0·23	0·14	0·13	0·05	0·16	0·02	0·00	0·00	0·05	0·04	0·01	0·04	0·42	0·03	0·01	0·000000

[normalized to primitive mantle after Hofmann (1988)] for representative crustal samples are compared with Neogene tholeiites from Gran Canaria and MORB in Fig. 4a. Of the crustal samples, the gabbros have lower incompatible element abundances than the basalts. All crustal samples have lower abundances of highly and moderately incompatible immobile elements than the Neogene tholeiites and have nearly flat patterns of the mildly incompatible elements, in contrast to the steep patterns of the Neogene tholeiites, which cross over the crustal patterns for Y and the HREE from Tb to Yb. The crustal samples, however, have similar incompatible element abundances to MORB, which also have flat HREE patterns. The shapes of the incompatible element patterns for some basalt samples (e.g. 303906) are remarkably similar to those for basalts from HIMU ocean islands such as St Helena (Fig. 4b).

Sr–Nd–Pb isotope data are presented in Table 2 for ocean crust samples from Gran Canaria and a tholeiitic gabbro xenolith in the 1949 eruption on La Palma. Samples from Gran Canaria and La Palma form an elongated, horizontal field in the Sr vs Nd isotope correlation diagram (Fig. 5), which overlaps the field for fresh samples of Atlantic MORB. In contrast to the $^{143}Nd/^{144}Nd$ ratio (0·51294–0·512306), which falls completely within the range for Atlantic N-MORB, the $^{87}Sr/^{86}Sr$ ratio (0·7029–0·7052) exhibits a relatively large range extending from the N-MORB field to values that are significantly more radiogenic. The Sr and Nd isotopic composition of the Gran Canaria samples is similar to the composition of altered (120 Ma) upper oceanic crust in the western Atlantic (Fig. 5; Staudigel *et al.*, 1995). A fresh plagioclase mineral separate from sample B914 has a value of 0·70288, which plots within the field for Atlantic N-MORB. The $^{87}Sr/^{86}Sr$ isotope ratio correlates positively with H_2O content [data from Schmincke *et al.* (1998)]. Leaching experiments were carried out on three samples (303903, 303905 and 303906) with high $^{87}Sr/^{86}Sr$ and high H_2O. After acid-washing, the residues yielded significantly lower Sr isotope ratios but Nd isotope ratios within analytical error (see Table 2 and Fig. 5).

The Sm–Nd data define an isochron with an age of 178 ± 17 Ma (1σ) with a mean square weighted deviate (MSWD) of 2·52 (Fig. 6) and an initial $^{143}Nd/^{144}Nd$ ratio of 0·51277. The $^{143}Nd/^{144}Nd$ ratio does not correlate with 1/Sm, ruling out the possibility of two-component mixing to explain the variation in Nd isotope ratio. The Sm–Nd age data, as well as $^{40}Ar/^{39}Ar$ single- and multiple-crystal laser dates of plagioclase (164 ± 3 Ma) and hornblende (173 ± 1 Ma) (Schmincke *et al.*, 1998), provide the strongest evidence that these samples are from the Jurassic oceanic crust and not the Canary plume.

The Pb isotope ratios for whole-rock samples from Gran Canaria exhibit extreme variation: $^{206}Pb/^{204}Pb$ = 18·2–20·8, $^{207}Pb/^{204}Pb$ = 15·59–15·73, $^{208}Pb/^{204}Pb$ = 38·1–41·3 (Fig. 7). Surprisingly, analyses of three different portions of a single basalt sample (B9117) yielded almost the entire observed range (Table 2b). The $^{206}Pb/^{204}Pb$ and $^{208}Pb/^{204}Pb$ isotope ratios for these three samples correlate positively with the degree of hydrothermal alteration. In the Pb isotope diagrams, almost all samples plot above the field for Atlantic N-MORB and the Northern Hemisphere Reference Line [NHRL, from Hart (1984)]. Sample B9117.3 with the highest $^{206}Pb/^{204}Pb$ plots slightly below the NHRL in the $^{207}Pb/^{204}Pb$ diagram, within the field for St Helena. The entire whole-rock data set, in particular the data for B9117 samples, falls within error of a line with a slope (0·049) equivalent to an age of 170 Ma, in agreement with the ages determined from Sm–Nd and Ar–Ar isotope systematics. In the thorogenic Pb isotope diagram, the data for sample B9117 form a line with a slope equivalent to Th/U of 3·8 (κ = 3·9).

The initial Pb isotope data for whole-rock samples fall between or within the fields for Atlantic N-MORB and sediments (Fig. 7b). Whole-rock sample B913 and the fresh plagioclase separate from B914 are within error of Jurassic Atlantic N-MORB. The whole-rock sample for B914, which contains secondary phases (such as actinolite, chlorite and sulfide) indicative of hydrothermal alteration, has similar initial $^{206}Pb/^{204}Pb$ but significantly higher initial $^{207}Pb/^{204}Pb$ and $^{208}Pb/^{204}Pb$, and is displaced towards the sediment field.

DISCUSSION

Effect of post-exhumation alteration on U and Pb concentrations

Alteration occurring after exhumation of the crustal samples on Gran Canaria (e.g. alteration related to the formation of the fanglomerate containing the crustal samples and post-depositional circulation of groundwater or hydrothermal fluids associated with later magmatic activity at Gran Canaria) has affected the concentration of some elements, as is best illustrated by sample B9117. The initial Pb isotope data for the three portions of B9117 show relatively large differences (e.g. $^{206}Pb/^{204}Pb$ ranges from 17·9 to 19·0). Several observations suggest that the μ and κ ratios, calculated from the measured U, Th and Pb concentrations, of samples B9117.2 and B9117.3 do not reflect the long-term, time-integrated ratios. First, the initial Sr and Nd isotope data for the three portions of B9117 are within error of each other. Second, the Pb isotope data for these samples fall within error of a 170 Ma reference isochron (Fig. 7a). Third, the excellent linear correlation in the $^{206}Pb/^{204}Pb$ vs $^{208}Pb/^{204}Pb$ diagram indicates that the time-integrated κ for these samples was 3·9 (Th/U = 3·8). Only sample

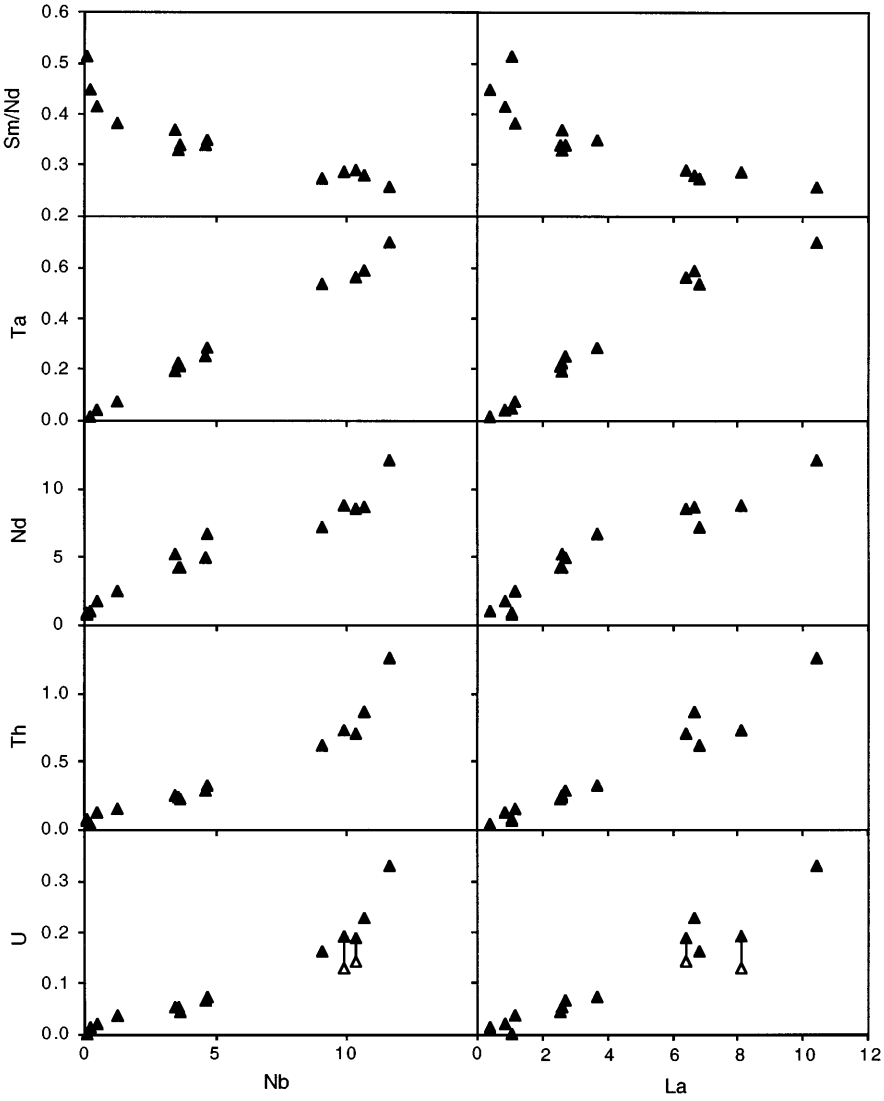

Fig. 2. Correlations between immobile incompatible trace elements for igneous samples from the Gran Canaria oceanic crust. The estimated U concentrations (▲; Table 3) for samples B9117.2 and B9117.3 before they were brought to the surface at ~14 Ma are connected to the measured values (△; Table 1).

B9117.1 has a κ of 3·9; samples B9117.2 and B9117.3 have substantially higher κ values of 5·2 and 5·9, respectively. These observations suggest that the initial Pb isotope ratios were similar and that recent mobilization of U, Th and/or Pb has occurred.

Under oxidizing conditions U can have a valence of 6^+, forming the uranyl ion (UO_2^{2+}). As the uranyl ion forms compounds that are soluble in water, it becomes highly mobile under oxidizing conditions. Th, on the other hand, only occurs in the tetravalent state and thus forms compounds that are generally insoluble in water (Faure, 1986). Assuming that Th has not been mobilized during alteration, the time-integrated U concentration can be estimated using the measured Th and the inferred time-integrated Th/U ratio of 3·8. On plots of U vs immobile elements, such as Nb, Ta and REE (e.g. Fig. 2), the estimated U concentrations (Table 3) for samples B9117.2 and B9117.3 plot closer to the trends formed by the other samples than the measured U concentrations. A plot of Th vs U for whole-rock samples suggests that all crustal samples may originally have had a Th/U ratio of ~3·8 (Fig. 3).

Using these U concentrations, we see that the initial Pb isotope ratios (using an age of 170 Ma) are much closer, but they are still outside error of each other. Recent hydrothermal alteration, associated with volcanism on Gran Canaria, may also have affected the Pb concentrations of samples B9117.2 and B9117.3. If we es-

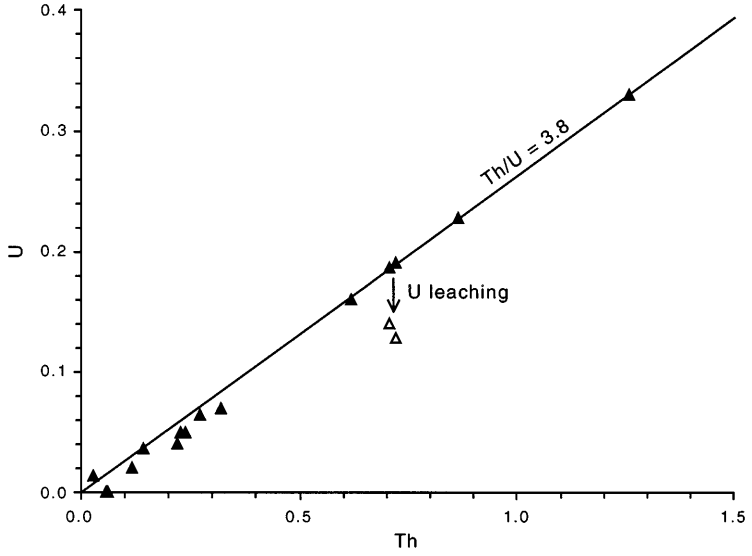

Fig. 3. Th vs U for ocean crust samples. Symbols same as in Fig. 2.

timate Pb concentrations for samples B9117.2 and B9117.3 by assuming that these samples have the same initial $^{208}Pb/^{204}Pb$ isotope composition as sample B9117.1, then the $^{206}Pb/^{204}Pb$ and $^{207}Pb/^{204}Pb$ isotope ratios for all three samples are within error (Table 3). In conclusion, post-exhumation alteration appears to have removed U and added Pb, resulting in an increase in κ and a decrease in μ in some but not all samples. Pre-exhumation μ and Ce/Pb ratios were as high as 107 and 134, respectively, as is illustrated by samples B9117.2 and B9117.3 (Table 3).

Effect of seafloor alteration–metamorphism and aging on trace element and isotopic compositions of oceanic crust

Both hydrothermal alteration–metamorphism and low-temperature alteration occur within the igneous portion of the oceanic crust. In normal oceanic crust, hydrothermal alteration will occur as long as the newly formed crust is near the ridge axis. An age of 10 Ma is probably a reasonable upper limit for hydrothermal alteration (Staudigel *et al.*, 1981), in the absence of later seamount or ocean island volcanism. In contrast, low-temperature alteration will continue, although at low rates, as long as there is sufficient permeability within the crust.

A number of observations indicate that neither metamorphism nor later low-temperature alteration affects the Nd isotopic system. First, the Sm and Nd abundances and the Sm/Nd and $^{143}Nd/^{144}Nd$ ratios correlate with immobile elements (e.g. Fig. 2). Second, leaching of three greenschist facies samples with an aqua regia solution did not change the $^{143}Nd/^{144}Nd$ isotope ratio outside error (Fig. 5). Third, the good correlation between $^{147}Sm/^{144}Nd$ and $^{143}Nd/^{144}Nd$ has a slope equivalent to an age of 178 $\pm$ 17 Ma (Fig. 6), similar to that expected from seafloor paleomagnetic data in the region and obtained by $^{40}Ar/^{39}Ar$ age dating. The $^{147}Sm/^{144}Nd$ ratios range from 0·15 to 0·27 in the whole rocks, resulting in an increase of up to 0·0003 in the $^{143}Nd/^{144}Nd$ ratio over 178 my.

The $^{87}Sr/^{86}Sr$ isotope ratios for all three B9117 samples and sample B914 fall within the field for Atlantic N-MORB (Fig. 5 and Table 2). Seawater alteration, however, has increased the Sr isotopic composition of the other samples (0·7037–0·7052), reflecting high water/rock ratios. Not only do the residues of all three leached samples have significantly lower $^{87}Sr/^{86}Sr$ than the unleached residues (Fig. 5), but the $^{87}Sr/^{86}Sr$ isotope ratio also correlates positively with H_2O content. In addition, the lack of correlation of Rb and Sr with immobile elements reflects the high mobility of both of these elements. The measured $^{87}Rb/^{86}Sr$ ratios range from 0·01 to 0·13, correlating with a maximum increase of 0·0003 in $^{87}Sr/^{86}Sr$. The fresh samples have the lowest $^{87}Rb/^{86}Sr$ ratios, whereas the altered samples have the highest ratios.

Both hydrothermal alteration and radiogenic ingrowth have played a major role in the evolution of the Pb isotope systematics. In Pb isotope diagrams, most of the crustal data plot above the field for Jurassic Atlantic N-MORB (Fig. 7b). Although it cannot be ruled out that the source for the Jurassic ocean crust beneath Gran Canaria had higher $^{207}Pb/^{204}Pb$ and $^{208}Pb/^{204}Pb$ than

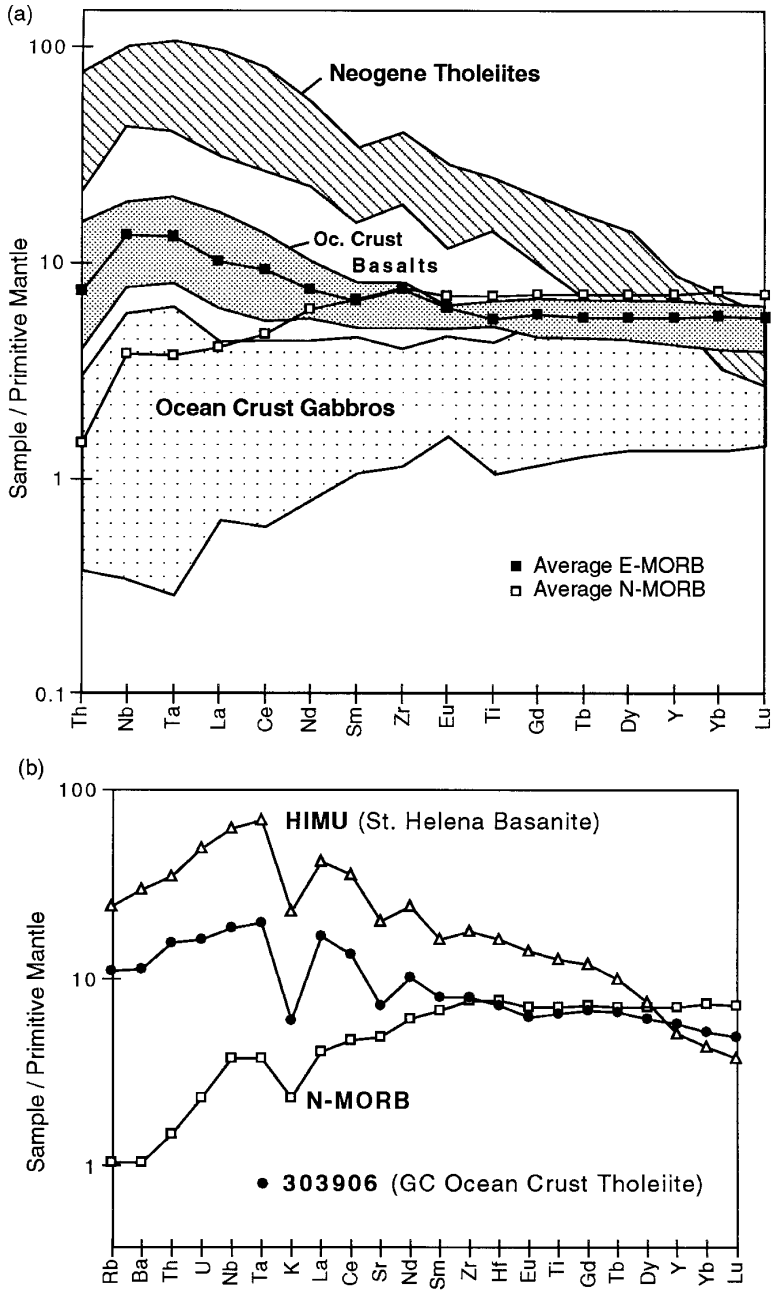

Fig. 4. Incompatible multi-element diagrams normalized to primitive mantle (Hofmann, 1988). (a) Immobile incompatible elements of tholeiitic basalts and gabbros from the ocean crust beneath Gran Canaria [data from Table 1 and Schmincke *et al.* (1998) for Zr and Ti] are compared with Miocene and Pliocene plume-derived tholeiites from Gran Canaria (Hoernle & Schmincke, 1993*a*) and with average enriched (E)-MORB and normal (N)-MORB from Sun & McDonough (1989). (b) As illustrated by tholeiitic basalt sample 303906, some Gran Canaria ocean crust samples have similar incompatible element characteristics to HIMU basanites from St Helena [sample 68 from Chaffey *et al.* (1989)].

most depleted mantle, comparison of the Pb isotopic composition of the fresh plagioclase separate with the altered whole rock for B914 suggests that hydrothermal alteration played a role in elevating these ratios. The initial Pb isotopic composition for the plagioclase separate falls within the field for Jurassic N-MORB in both Pb isotope diagrams, whereas the altered whole-rock sample has similar $^{206}Pb/^{204}Pb$ but significantly higher $^{207}Pb/^{204}Pb$ and $^{208}Pb/^{204}Pb$. This relationship is consistent with hydrothermal alteration adding a crustal Pb component

Table 2: Isotopic data for Gran Canaria ocean crust samples and one gabbro xenolith in the 1949 eruption on La Palma
(a) Sr and Nd isotopic data

		$^{87}Sr/^{86}Sr$	$^{87}Rb/^{86}Sr$	$(^{87}Sr/^{86}Sr)_T$	$^{143}Nd/^{144}Nd$	ε_{Nd}	$^{147}Sm/^{144}Nd$	$(^{143}Nd/^{144}Nd)_T$	$\varepsilon_{Nd(T)}$
Gran Canaria									
Sediment layer 1									
917c	whole-rock	0·709643(19)	0·81	0·70768	0·511985(3)	−12·7	0·12	0·51185	−11·2
91249	whole-rock	0·715426(13)	1·11	0·71275	0·511978(5)	−12·9	0·13	0·51183	−11·4
DSDP397-60-4	whole-rock	0·710291(12)	1·21	0·70737	0·511965(7)	−13·1	0·11	0·51184	−11·3
DSDP397-101-1	whole-rock	0·723619(13)	0·09	0·72340	0·512080(7)	−10·9	0·11	0·51196	−9·03
DSDP397-30-1	whole-rock	0·709362(23)	1·48	0·70579	0·511664(12)	−19·0	0·11	0·51154	−17·2
DSDP397-40-2	whole-rock	0·709363(16)	0·12	0·70908	0·512131(6)	−9·89	0·11	0·51201	−8·08
DSDP397-49-1	whole-rock	0·709288(25)	0·11	0·70903	0·512157(8)	−9·38	0·11	0·51203	−7·52
Basalt layer 2									
303905	whole-rock	0·705243(10)	0·02	0·70520	0·513004(8)	7·14	0·21	0·51277	6·89
303905 a.w.	acid-washed	0·704716(10)			0·513032(18)				
303906	whole-rock	0·704004(8)	0·14	0·70367	0·512949(9)	6·07	0·15	0·51278	7·00
303906 a.w.	acid-washed	0·703822(14)			0·512935(10)				
B9117.1	whole-rock	0·702862(13)	0·01	0·70283	0·512965(4)	6·38	0·17	0·51278	7·01
B9117.2	whole-rock	0·702859(11)	0·01	0·70283	0·512962(11)	6·32	0·17	0·51277	6·83
B9117.3	whole-rock	0·702923(17)	0·02	0·70288	0·512954(25)	6·16	0·17	0·51276	6·72
Gabbro layer 3									
303903	whole-rock	0·703716(14)	0·01	0·70368	0·513042(11)	7·88	0·22	0·51280	7·36
303903 a.w.	acid-washed	0·703146(21)			0·513026(18)				
B913	whole-rock	0·704399(14)	0·11	0·70413	0·512958(10)	6·24	0·16	0·51278	6·96
B914	whole-rock	0·702992(28)	0·06	0·70284	0·513061(8)	8·26	0·25	0·51279	7·15
B914	plagioclase	0·702879(21)	0·01	0·70284	0·512938(15)	5·85	0·13	0·51280	7·36
La Palma (gabbro)									
241921B	whole-rock	0·703272(13)	0·08	0·70310	0·512980(8)	6·67	0·17	0·51281	6·67

Table 2: Isotopic data for Gran Canaria ocean crust samples and one gabbro xenolith in the 1949 eruption on La Palma
(b) Pb isotopic data

	$^{206}Pb/^{204}Pb$	$^{207}Pb/^{204}Pb$	$^{208}Pb/^{204}Pb$	μ	κ	$(^{206}Pb/^{204}Pb)_T$	$(^{207}Pb/^{204}Pb)_T$	$(^{208}Pb/^{204}Pb)_T$
Gran Canaria								
Sediment layer 1								
917c	19·059	15·699	39·299	8·67	7·20	18·83	15·69	38·77
91249	18·922	15·700	39·177	1·31	6·09	18·89	15·70	39·11
DSDP397-60-4	19·018	15·745	39·201	6·57	4·40	18·84	15·74	38·96
DSDP397-101-1	18·903	15·699	39·092	21·4	1·68	18·33	15·67	38·79
DSDP397-30-1	18·975	15·726	39·015	10·4	3·40	18·70	15·71	38·72
DSDP397-40-2	18·949	15·701	39·183	17·6	2·16	18·48	15·68	38·86
DSDP397-49-1	18·951	15·695	39·182	15·3	2·61	18·54	15·68	38·85
Basalt layer 2								
303905	18·155	15·605	38·078	14·2	4·72	17·77	15·59	37·51
303906	18·385	15·597	38·246	5·87	3·95	18·23	15·59	38·05
B9117.1	18·443	15·596	38·456	21·6	3·94	17·87	15·57	37·74
B9117.1	18·447	15·580	38·401					
B9117.2	19·357	15·663	39·553	25·4	5·23	18·68	15·63	38·43
B9117.3	20·753	15·728	41·303	65·5	5·87	19·00	15·64	38·06
Gabbro layer 3								
303903	18·221	15·591	38·097	5·83	4·96	18·06	15·58	37·85
B913	19·067	15·620	38·841	5·30	4·00	18·93	15·61	38·66
B914 w.r.	18·664	15·638	38·486	3·11	6·20	18·58	15·63	38·32
B914 plag.	18·545	15·576	38·255	0·00		18·54	15·58	38·03
Pliocene basalts								
RNB60	18·994	15·525	39·039					
RN1249	18·931	15·509	38·988	24·9	4·63	18·91	15·51	38·96

Analyses of residues after boiling for 1 h in a mixture of 50% 6 N HCl and 50% 8 N HNO_3 are denoted as acid-washed (a.w.). The errors in parentheses after the measured isotope ratios are 2σ and pertain to the last digits. Sr blanks measured during this study were <300 pg; Pb and Nd blanks were $\leq$100 pg. Age corrections were made using an age (T) of 170 Ma for all samples, except for the La Palma gabbro (T = 156 Ma). Initial Sr–Nd–Pb isotopic data for sediment samples from DSDP Site 397 (using the age of deposition) and Sr and Nd isotope data for RN1249 and RNB60 samples, as well as Pb, U and Th concentrations for RN1249, have been presented by Hoernle *et al.* (1991).

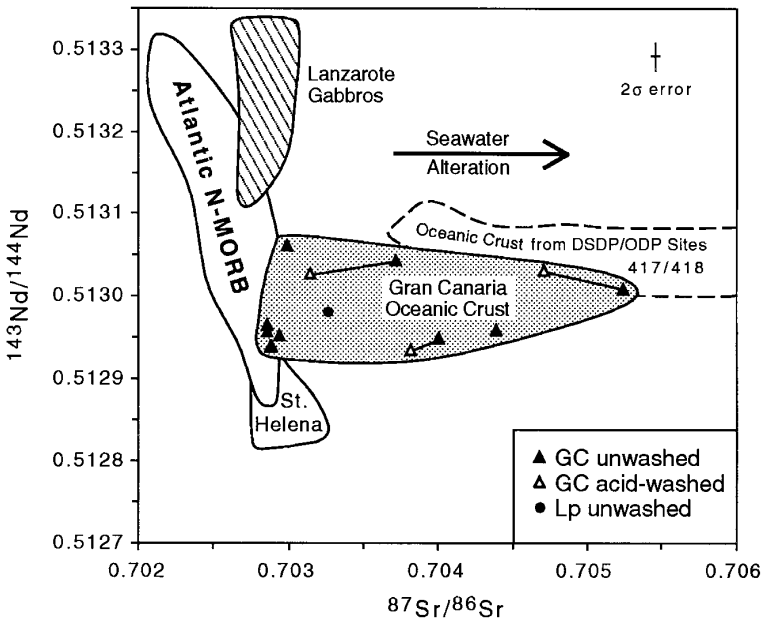

Fig. 5. $^{87}Sr/^{86}Sr$ (measured) vs $^{143}Nd/^{144}Nd$ (measured) isotope correlation diagram for Balos ocean crust samples from Gran Canaria (triangles), a tholeiitic gabbro xenolith from the 1949 eruption on La Palma (circle), and the field for Lanzarote tholeiitic gabbro xenoliths (Vance *et al.*, 1989; E.-R. Neumann & M. Whitehouse, unpublished data), showing that oceanic crust is present beneath the entire Canary Island chain. After boiling samples from Gran Canaria for 1 h in a mixture of 50% 6 N HCl and 50% 8 N HNO_3, residues (△) have lower Sr but similar Nd isotopic compositions, illustrating the effects of seawater alteration. Also shown are fields for (1) Atlantic N-MORB between 30°N and 6°S, excluding area influenced by Sierra Leone hotspot (1–3°N) (Ito *et al.*, 1987; Dosso *et al.*, 1991; Schilling *et al.*, 1994), (2) St Helena (Chaffey *et al.*, 1989), and (3) composites of the upper ~800 m of ~120 Ma ocean crust from DSDP–ODP Sites 417 and 418 in the western Atlantic (Staudigel *et al.*, 1995).

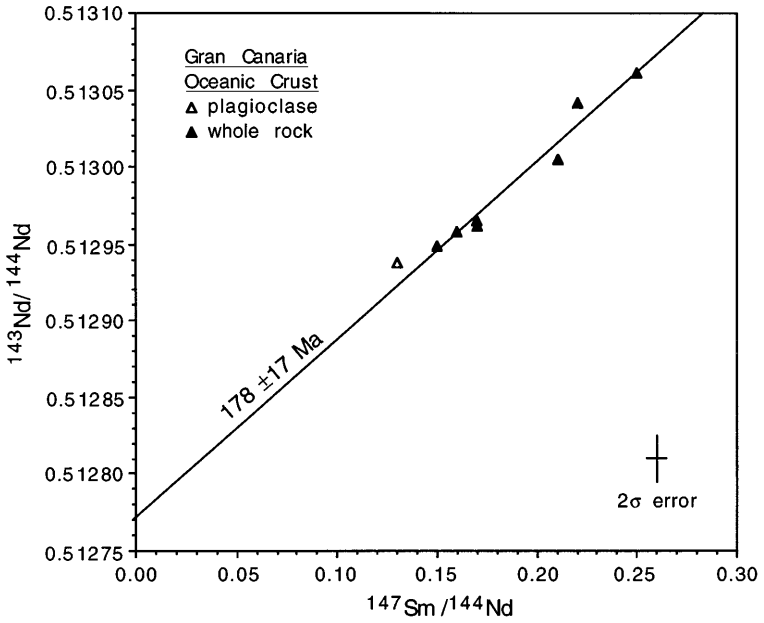

Fig. 6. In the $^{147}Sm/^{144}Nd$ vs $^{143}Nd/^{144}Nd$ diagram, the Balos whole-rock and plagioclase samples define an isochron with an age of 178 ± 17 Ma (1σ) with a mean square weighted deviate (MSWD) of 2·52 and an initial $^{143}Nd/^{144}Nd$ ratio of 0·51277. An age of 178 ± 17 Ma agrees well with that inferred from paleomagnetic data (see Fig. 1).

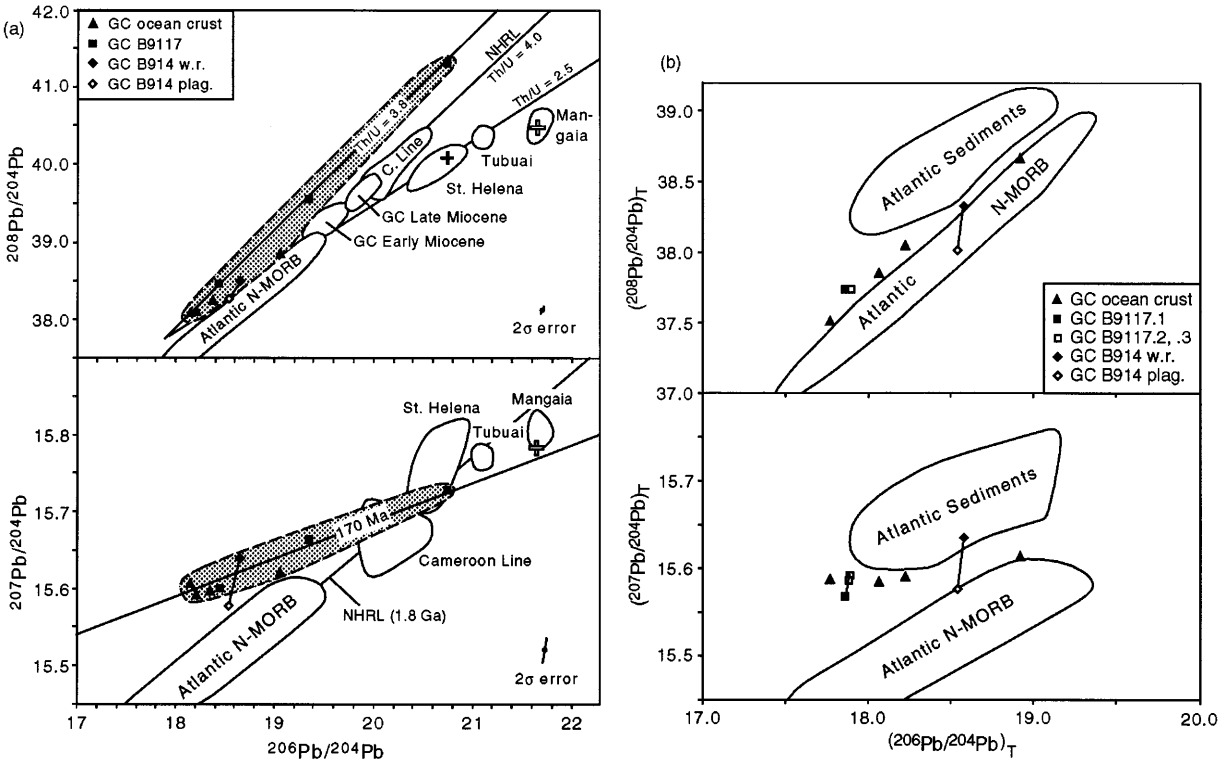

Fig. 7. (a) Measured Pb isotope ratios for the oceanic crust beneath Gran Canaria (from Table 2). In the $^{206}Pb/^{204}Pb$ and $^{207}Pb/^{204}Pb$ diagram, the whole-rock data fall within error of a 170 Ma reference isochron; whereas in the $^{206}Pb/^{204}Pb$ vs $^{208}Pb/^{204}Pb$ isotope diagram, the samples form an array with Th/U of ~3·8. In the uranogenic Pb diagram, all samples except B9117.3 lie above the field for Atlantic N-MORB and the Northern Hemisphere Reference Line (NHRL; Hart, 1984). Sample B9117.3 has $^{206}Pb/^{204}Pb$ and $^{207}Pb/^{204}Pb$ ratios similar to those for basalts from St Helena, the Atlantic type locality for the HIMU component in ocean islands. The $^{208}Pb/^{204}Pb$ ratio, however, is significantly higher. As shown in the thorogenic diagram (solid cross), a $^{208}Pb/^{204}Pb$ ratio similar to that for St Helena samples could have been generated if the Th/U ratio had been 2·5 instead of 3·8 over the last 170 my. Compositions (open cross) similar to those of lavas from Mangaia, the most extreme example of HIMU in ocean islands, could evolve if portions of the crust similar to sample B9117.3 were allowed to age another 50 my and if the crust had Th/U = 2·2 over its entire ~220 my life-span (i.e. since formation at a mid-ocean ridge). Fields for the Gran Canaria Early and Late Miocene volcanic rocks are shown in the thorogenic Pb isotope diagram. (b) Initial Pb isotope data. In both Pb isotope diagrams, the data corrected for *in situ* decay fall between the fields estimated for Jurassic Atlantic N-MORB (assuming $\mu = 5$ and $\kappa = 2{\cdot}5$ for the depleted mantle, i.e. MORB source; see White, 1993) and Jurassic Atlantic oceanic sediments (using the μ and κ measured in each sample). Magmatic plagioclase from sample B914 falls within the field for N-MORB in both Pb isotope diagrams, whereas the hydrothermally altered whole-rock has higher $^{207}Pb/^{204}Pb$ and $^{208}Pb/^{204}Pb$ ratios, which plot within or just below the field for oceanic sediments. The high $^{207}Pb/^{204}Pb$ and $^{208}Pb/^{204}Pb$ (and high $\Delta 7/4Pb$ and $\Delta 8/4Pb$) in the whole-rock samples are consistent with the addition of crustal Pb from oceanic sediments to the Jurassic oceanic crust by hydrothermal alteration. The initial Pb isotope ratios for samples B9117.2 and B9117.3 are from Table 3. Data sources not given in Fig. 5 are as follows: N-MORB and sediments (Sun, 1980; Ben Othman *et al.*, 1989; Hoernle *et al.*, 1991), Mangaia (Nakamura & Tatsumoto, 1988), Tubuai (Vidal *et al.*, 1984) and Cameroon Line (Halliday *et al.*, 1988, 1990).

Table 3: Pre-exhumation (>14 Ma) Pb (ppm), U (ppm), μ, initial $^{206}Pb/^{204}Pb$ and initial $^{207}Pb/^{204}Pb$ for ocean crust basalt samples B9117.2 and B9117.3

	Pb	U	Nb/U	Ce/Pb	$^{206}Pb/^{204}Pb$	$^{207}Pb/^{204}Pb$	μ	$(^{206}Pb/^{204}Pb)_T$	$(^{207}Pb/^{204}Pb)_T$
B9117.1	0·67	0·23	47	21	18·44	15·60	22	17·87	15·57
B9117.2	0·22	0·19	56	62	19·36	15·66	55	17·90	15·59
B9117.3	0·12	0·19	52	133	20·75	15·73	107	17·89	15·59

Values were estimated using an age (*T*) of 170 Ma and assuming that samples B9117.2 and B9117.3 have the same κ (3·94) and initial $^{208}Pb/^{204}Pb$ (37·74) as sample B9117.1. A value of 3·94 for κ was also inferred for all three B9117 samples from the slope of these data on the thorogenic Pb isotope diagram (Fig. 7a). Measured Nb and Ce concentrations (Table 1) were used to calculate pre-exhumation Nb/U and Ce/Pb ratios. Measured $^{206}Pb/^{204}Pb$ amd $^{207}Pb/^{204}Pb$ are from Table 2(b)

(derived from oceanic sediments) to the igneous ocean crust (Hanan & Graham, 1996).

Hydrothermal alteration can also affect the U/Pb, Th/Pb and Ce/Pb ratios but does not appear to significantly fractionate Th/U or Nb/U. Neither Nb or Ce appears to be significantly affected by seafloor metamorphism, as is evident from the good correlation between these elements and other immobile elements (e.g. Fig. 2; also Staudigel *et al.*, 1995). If Nb/U is 47 $\pm$ 10 and Ce/Pb is 25 $\pm$ 5 in fresh MORB as proposed by Hofmann *et al.* (1986), then we can estimate the original U/Pb (and μ) ratios for these samples. The estimated μ ratios (18–26, excluding coarse-grained gabbros) show only minor variation, falling within the upper range for MORB (2–25; White, 1993). As is illustrated by sample B9117 (Table 3), hydrothermal alteration near the ridge axis can substantially raise μ and Ce/Pb ratios (to values as high as 107 and 133, respectively) but does not appear to have significantly affected Nb/U (47–56) or Th/U (3·8), suggesting that the high μ and Ce/Pb ratios in the altered samples primarily reflect Pb loss. The high Th/U ratio and the enriched abundances of immobile incompatible elements in basaltic samples, as well as the HIMU-type incompatible element characteristics in some samples, may reflect the presence of young (<0·5 Ga) recycled oceanic crust in the source of the Jurassic oceanic crust (Figs 3 and 4b).

After hydrothermal alteration near the mid-ocean ridge, it is unlikely that the Pb isotopic composition will be significantly affected by subsequent low-temperature seawater alteration, because of the low concentration of Pb in cold seawater (e.g. Faure, 1986). During this second evolutionary stage of ocean crust ($\leq$10 Ma until subduction), the Pb isotopic composition will primarily change as a result of radiogenic ingrowth, especially in portions of the crust with extremely high μ values of 55 (B9117.2) or 107 (B9117.3). Radiogenic ingrowth will not only result in the isotopic composition of the crust becoming more radiogenic but will also serve to widen the isotopic range of the crust (increase its heterogeneity), especially in older ($\geqslant$100 my) ocean crust.

In summary, the ocean crust beneath Gran Canaria had an Sr, Nd and Pb isotopic composition ~170 my ago similar to that expected for the Jurassic MORB source (depleted mantle). Hydrothermal alteration near the ridge axis, subsequent low-temperature alteration and radiogenic ingrowth, however, have significantly changed the Sr and Pb isotopic compositions and U/Pb, Th/Pb and Ce/Pb ratios in the oceanic crust beneath Gran Canaria from that of present-day MORB.

Constraints on the age of recycled ocean crust and the HIMU component in ocean islands

Age constraints for the recycling of oceanic crust through a subduction zone are primarily based on the Pb isotope systematics of ocean islands with the most radiogenic Pb or HIMU-type compositions. Recycling times for end-member HIMU ocean islands are generally believed to be ~2 gy, although recently Hanan & Graham (1996), with a model similar to the one presented in this study, proposed that it may be possible to generate St Helena type HIMU within 300 my. It is clear from this study that old altered ocean crust can have HIMU-type trace element characteristics (Fig. 4b) and Sr–Nd–Pb isotopic compositions even before subduction. For example, sample B9117.3 has $^{87}Sr/^{86}Sr$ (0·7029), $^{143}Nd/^{144}Nd$ (0·51295), $^{206}Pb/^{204}Pb$ (20·8) and $^{207}Pb/^{204}Pb$ (15·73) similar to present-day samples from St Helena ($^{87}Sr/^{86}Sr$ = 0·7028–0·7032, $^{143}Nd/^{144}Nd$ = 0·51282–0·51297, $^{206}Pb/^{204}Pb$ = 20·4–20·9 and $^{207}Pb/^{204}Pb$ = 15·71–15·81; Chaffey *et al.*, 1989). Sample B9117.3, however, is distinct from HIMU-type OIB in having even more radiogenic $^{208}Pb/^{204}Pb$ (41·3) than St Helena (39·7–40·2) and all other end-member HIMU ocean islands (see Fig. 7a). The higher $^{208}Pb/^{204}Pb$ ratio for B9117.3 reflects a high time-integrated Th/U of 3·8, which falls at the upper end of Th/U found in MORB (e.g. ~1·2–4·3; White, 1993). If sample B9117.3 had a Th/U of 2·5 (an average value for MORB) instead of 3·8, then it would at present have a $^{208}Pb/^{204}Pb$ ratio of 40·1, within the range for St Helena (solid cross in Fig. 7a), instead of the measured value of 41·3.

Even though the crust beneath the Canary Islands is about the oldest *in situ* oceanic crust that exists at present, it will probably be significantly older before it is subducted, because of its location on a passive margin. If other portions of the crust in the vicinity of the Canary Islands have the same Pb isotopic composition and μ as sample B9117 and κ of 2·4, they will evolve Pb isotope ratios similar to those for Mangaia (see Fig. 7a), with the most extreme Pb isotopic or HIMU-like composition of all ocean islands, in another 53 my (or when the age of the crust is ~223 Ma). If the ocean crust along the NW African and Iberian margins ages beyond 223 Ma before it is subducted, even more extreme Pb isotopic compositions could be generated than those for Mangaia.

Although intermediate compositions are often explained through mixing between end-members, the Cameroon Line end-member cannot be derived through mixing of HIMU (defined by either St Helena or Mangaia) and MORB in the thorogenic Pb diagram (Fig. 7a). However, assuming an initial Pb isotope composition similar to whole-rock sample B914 (Table 2) and a μ and κ similar to those estimated for B9117.3 (Table 3), the Cameroon Line samples with the most radiogenic Pb could be generated within 115 my.

Even though the most extreme HIMU can be generated within 223 my, these estimates reflect minimum ages, as the most extreme μ was used. Maximum ages can be calculated using the bulk composition of the crust (see next

section) and a minimum μ. The average pre-alteration μ (20), calculated assuming Nb/U = 47 and Ce/Pb = 25, serves as a minimum value, because hydrothermal alteration near the ridge axis (as discussed above) and subduction are both likely to increase μ (e.g. Hart & Staudigel, 1989; Kogiso *et al.*, 1997). Therefore, maximum ages for generating end-member HIMU from Gran Canaria ocean crust are ~740 Ma for the Cameroon Line, ~770 Ma for St Helena and ~1070 Ma for Mangaia.

Composition of oceanic crust: implications for OIB sources

The oceanic crust beneath Gran Canaria consists of two major units: an igneous unit (4·5 km thick; layers 2 and 3) overlain by a sedimentary unit (up to 6 km thick; layer 1). The igneous portion of the crust (layers 2 and 3) has the following average trace element abundances and isotope ratios (weighted to trace element abundances) for the samples analyzed for isotope ratios: Sr = 106 ppm, $^{87}Sr/^{86}Sr$ = 0·70362, Nd = 7·3 ppm, $^{143}Nd/^{144}Nd$ = 0·51298, Pb = 1 ppm, $^{206}Pb/^{204}Pb$ = 18·62, $^{207}Pb/^{204}Pb$ = 15·61 and $^{208}Pb/^{204}Pb$ = 38·49. The sedimentary portion of the crust (layer 1) has these average values: Sr = 612 ppm, $^{87}Sr/^{86}Sr$ = 0·71368, Nd = 16·9 ppm, $^{143}Nd/^{144}Nd$ = 0·51198, Pb = 12·1 ppm, $^{206}Pb/^{204}Pb$ = 18·97, $^{207}Pb/^{204}Pb$ = 15·72 and $^{208}Pb/^{204}Pb$ = 39·16 [Table 2 and Hoernle *et al.* (1991)]. In contrast to the mantle and mantle-derived melts, the oceanic crust beneath Gran Canaria extends to substantially more radiogenic Sr, less radiogenic Nd and higher $^{207}Pb/^{204}Pb$ and $^{208}Pb/^{204}Pb$ at a given $^{206}Pb/^{204}Pb$ (higher Δ7/4Pb and Δ8/4Pb). The sedimentary portion of the crust is more likely to create noticeable contamination of ascending magmas, because of its more extreme isotopic composition and higher Sr, Nd and Pb concentrations. The Nd isotopic ratio can be used to distinguish between contamination in different levels of the crust, as the sedimentary crust has extremely unradiogenic Nd and the igneous crust very radiogenic Nd.

Normal oceanic crust is 7·1 ± 0·8 km thick, although in some regions, for example Kolbeinsey Rise, it can reach thicknesses of up to 16 km (White *et al.*, 1992). In thicker oceanic crust, it is likely that two separate isotopic reservoirs may exist within the igneous crust: (1) an upper portion affected by alteration, including layer 2 and variable amounts of layer 3, and (2) the lower portion of layer 3 in thicker crust, which may remain unaffected by seafloor metamorphism and subsequent alteration. The upper, altered portion of the crust, especially if aged, can display a large range in both Sr and Pb isotopic composition. The crustal samples analyzed in this study cover 50% of the range in $^{87}Sr/^{86}Sr$ observed in OIB, 60% of the range in $^{206}Pb/^{204}Pb$ and a similar range in $^{208}Pb/^{204}Pb$, despite the small number of analyses (Fig. 8). The entire range in Pb isotopic composition found in OIB could have been generated in the sub-Canarian ocean crust if it were allowed to age another 50 my (see previous section) and if some portions contained low μ values. The highest $^{87}Sr/^{86}Sr$ isotopic ratios in OIB (up to 0·7074; Wright & White, 1987) have been found in basalts from Samoa. $^{87}Sr/^{86}Sr$ ratios as high as 0·7074 have been reported for altered oceanic crust (Staudigel *et al.*, 1995). Therefore the entire range in Pb and Sr isotopic composition observed in OIB could result from metamorphism and subsequent low-temperature alteration of igneous ocean crust.

Fresh portions of the mid to lower gabbro layer (layer 3) of thick oceanic crust could form a second reservoir with a composition similar to fresh MORB. This lower-crustal reservoir is likely to be more homogeneous in its trace element and isotopic composition than the altered, upper-crustal reservoir. Because of its MORB isotopic composition and lower μ values, it would take this reservoir significantly longer (2 gy) to evolve end-member HIMU-type Pb isotopic compositions (e.g. Sun, 1980; Silver *et al.*, 1988). Sr and Nd isotope ratios will probably range between DM and HIMU.

Both potential reservoirs within the igneous portion of the crust will have radiogenic Nd isotope ratios. Therefore, they cannot be a source for the low Nd isotope ratios in OIB (e.g. as low as 0·5123 at Walvis Ridge; Richardson *et al.*, 1982). Small amounts of sediments from layer 1 of the oceanic crust, however, could serve as the unradiogenic Nd end-member.

Crustal contamination of Neogene plume melts forming Gran Canaria

The Miocene or shield cycle of volcanism on Gran Canaria can be divided into two groups based on age and major element, trace element and isotopic composition: (1) Early Miocene group (~13·3–15 Ma) and (2) Late Miocene group (~10–13·3 Ma) (Cousens *et al.*, 1990; Hoernle *et al.*, 1991; Hoernle & Schmincke, 1993*a*, 1993*b*). The Early Miocene group has higher $^{87}Sr/^{86}Sr$ but lower $^{206}Pb/^{204}Pb$, $^{208}Pb/^{204}Pb$ and Ce/Pb ratios than the Late Miocene group; $^{143}Nd/^{144}Nd$ and $^{207}Pb/^{204}Pb$ ratios are indistinguishable between the two groups (e.g. Fig. 9). Early Miocene basalt samples analyzed for $\delta^{18}O_{cpx}$ fall within two groups: (1) low $\delta^{18}O_{cpx}$ (5·0–5·7‰), 15 samples, and (2) high $\delta^{18}O_{cpx}$ (6·0–6·8‰), three samples (Thirlwall *et al.*, 1997). Trachyte and rhyolite samples from the Early Miocene (four samples) and Late Miocene (one sample) have low average $\delta^{18}O_{fsp}$ (5·7–6·0‰; Crisp & Spera, 1987). The isotopic variations in Miocene volcanic rocks are interpreted as reflecting either (1) differences in the composition of the Miocene mantle

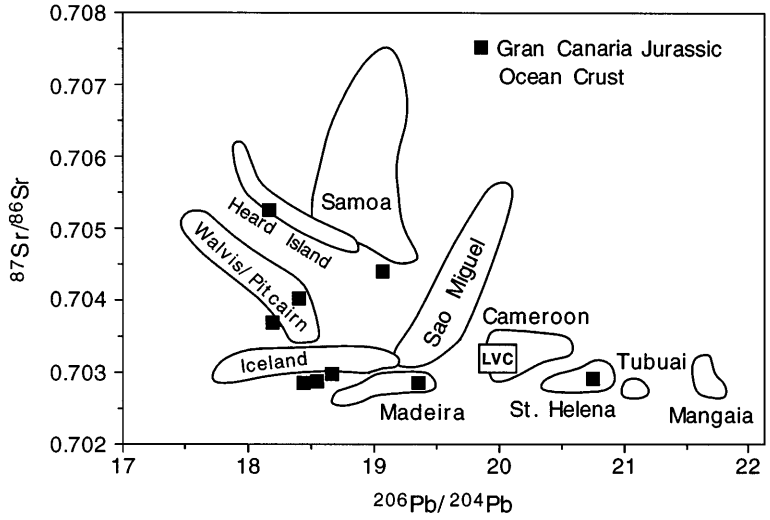

Fig. 8. Measured $^{206}Pb/^{204}Pb$ and $^{87}Sr/^{86}Sr$ isotope ratios for basalt and gabbro samples from the Jurassic ocean crust beneath Gran Canaria cover $\geq 50\%$ of the range observed in ocean island basalts. Data sources not listed in Figs 5 and 8 are as follows: LVC (low velocity component; Hoernle *et al.*, 1995), Madeira (Hoernle *et al.*, in preparation), São Miguel (Hawkesworth *et al.*, 1979; White *et al.*, 1979; Davies *et al.*, 1989; Widom *et al.*, 1998*a*), Iceland (Elliot *et al.*, 1991; Furman *et al.*, 1991), Walvis and Pitcairn (Richardson *et al.*, 1982; Woodhead & McCulloch, 1989), Heard Island (Storey *et al.*, 1988; Barling & Goldstein, 1990; Barling *et al.*, 1994) and Samoa (Wright & White, 1987).

sources (Cousens *et al.*, 1990; Hoernle *et al.*, 1991) or (2) crustal assimilation by mantle melts with uniform composition (Thirlwall *et al.*, 1997).

The three samples with high $\delta^{18}O_{cpx}$ also have the highest $^{87}Sr/^{86}Sr$, $^{207}Pb/^{204}Pb$ and $\Delta 7/4Pb$, and lowest $^{143}Nd/^{144}Nd$ ratios of all Miocene samples, consistent with assimilation of up to 8 wt % sediment. The other Early Miocene samples have probably assimilated <2 wt % sediment (Thirlwall *et al.*, 1997). When the three high $\delta^{18}O$ samples are excluded, the $\delta^{18}O_{cpx}$ values for the Miocene shield basalts show no obvious correlations with Sr or Nd isotope ratio but do show inverse correlations with $^{206}Pb/^{204}Pb$, Ce/Pb, Zr/Y, most incompatible elements (e.g. LREE, Nb, Th, Ti, Ba, Rb, P, K, Na, Sr) and Al_2O_3, and positive correlations with *mg*-number, MgO and CaO/Al_2O_3 [e.g. Fig. 10 and Thirlwall *et al.* (1997)]. Clinopyroxene from mantle peridotites yields a mean $\delta^{18}O$ value of $5{\cdot}57 \pm 0{\cdot}36‰$ (2 SD, $n = 57$) and ranges from 5·25 to 5·90‰ (Mattey *et al.*, 1994). The mean $\delta^{18}O_{ol}$ of $5{\cdot}30 \pm 0{\cdot}24‰$ (2 SD, $n = 25$) in mantle peridotites from the lithospheric mantle beneath the Canary and Madeira Islands (Wiechert *et al.*, in preparation) agrees well with the mean $\delta^{18}O_{cpx}$ for mantle peridotites using $\Delta cpx–ol = 0{\cdot}4‰$ (Mattey *et al.*, 1994). Therefore the Miocene samples (in the low $\delta^{18}O$ group), which have the highest $\delta^{18}O_{cpx}$ (up to 5·7‰), $^{206}Pb/^{204}Pb$ and *mg*-numbers, could have compositions similar to their mantle source(s).

Assimilation of hydrothermally altered (low $\delta^{18}O$) oceanic crust during fractional crystallization (AFC) of hot mantle-derived melts (Eiler *et al.*, 1996*a*, 1996*b*; Thirlwall *et al.*, 1997) is one possibility for explaining the decrease in *mg*-number and $\delta^{18}O$ (to values as low as 5·0‰ in cpx and 5·7‰ in plag) and the increase in incompatible element concentrations. Nevertheless, the inferred fractionating assemblage in these rocks, consisting of olivine (decrease in *mg*-number, MgO and Ni with decreasing $\delta^{18}O$) and clinopyroxene but not significant plagioclase (as indicated by the decrease in CaO/Al_2O_3 and increase in Al_2O_3, Na_2O and Sr with decreasing $\delta^{18}O$ and the lack of negative Eu anomaly), indicates that fractionation occurred within the mantle ($\geq$15–20 km depth) (Hoernle & Schmincke, 1993*a*). Therefore, if AFC caused the decrease in $\delta^{18}O$, it is likely to have occurred within the mantle instead of the crust.

Several additional observations also argue against a major role for shallow (<15 km) assimilation of igneous oceanic crust. As is illustrated in the Sr vs Nd (Fig. 9a) and the $^{206}Pb/^{204}Pb$ vs $^{208}Pb/^{204}Pb$ (Fig. 7a) isotope correlation diagrams, it is not possible to derive the Late Miocene group through assimilation of local ocean crust by mantle melts with a composition similar to the Early Miocene group. Furthermore, the Late Miocene volcanic rocks have compositions similar to the low velocity component (LVC), which is a plume component found throughout the eastern Atlantic, western Mediterranean and western and central Europe (Hoernle *et al.*, 1995). The $^{87}Sr/^{86}Sr$, $^{143}Nd/^{144}Nd$, $^{206}Pb/^{204}Pb$ and $^{207}Pb/^{204}Pb$ ratios of the Early Miocene group, however, could be explained through interaction of plume melts similar in composition to the Late Miocene group with altered, igneous ocean crust. As is illustrated by the mixing curves in Fig. 9, a

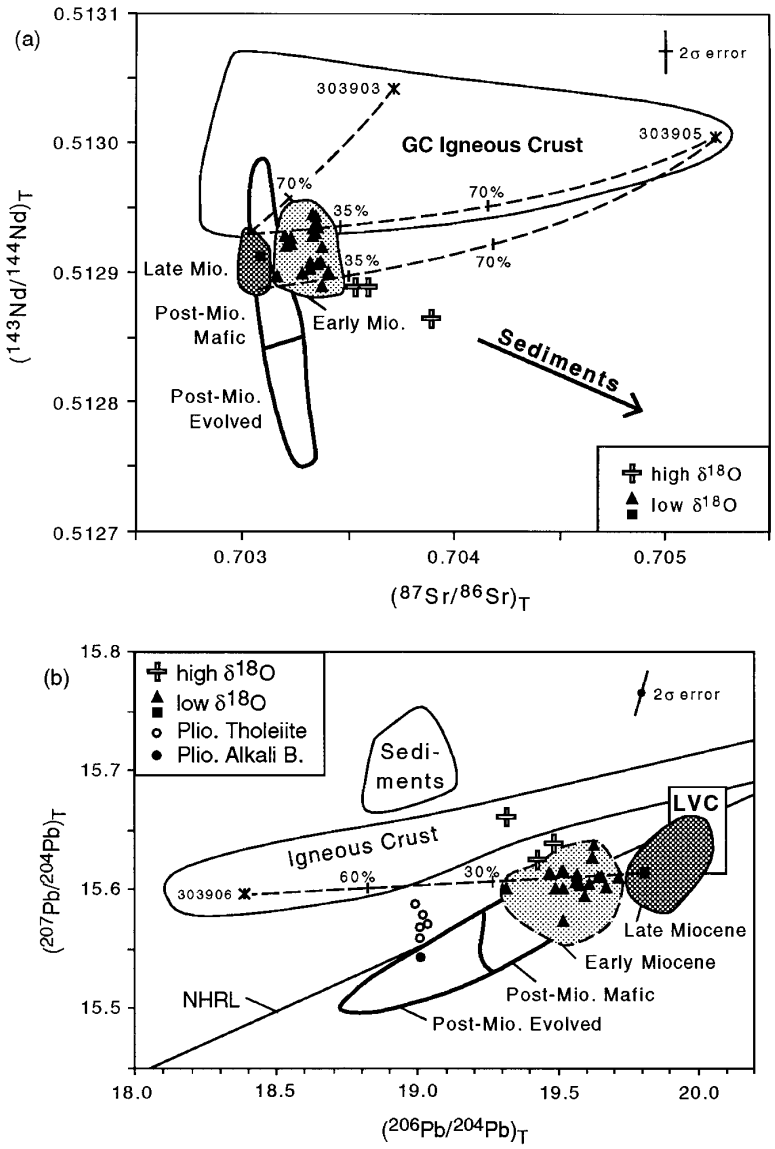

Fig. 9. Initial isotope data from Neogene Gran Canaria volcanic rocks are compared with present-day isotopic data for the Jurassic ocean crust beneath Gran Canaria in diagrams of (a) $^{87}Sr/^{86}Sr$ vs $^{143}Nd/^{144}Nd$ and (b) $^{206}Pb/^{204}Pb$ vs $^{207}Pb/^{204}Pb$ isotope ratios. The Early Miocene volcanic rocks have higher $^{87}Sr/^{86}Sr$ but lower $^{206}Pb/^{204}Pb$ than the Late Miocene volcanic rocks. The $\delta^{18}O$ data for the Miocene volcanic rocks can be divided into two groups: (1) Early Miocene basalts (crosses) with high $\delta^{18}O_{cpx}$ (6·0–6·8), and (2) basalts through highly evolved trachytes and peralkaline rhyolites (Early Miocene, triangle; Late Miocene, square) with low average $\delta^{18}O_{cpx}$ (5·0–5·7) and $\delta^{18}O_{fsp}$ (5·7–6·0). The three Early Miocene basalts with high $\delta^{18}O$ also have the most radiogenic Sr, least radiogenic Nd and highest $\Delta 7/4$Pb isotopic compositions, consistent with sediment assimilation (Thirlwall *et al.*, 1997). Mixing curves between the Late Miocene group and igneous crust are shown. For the Late Miocene end-member the trace element contents of the most depleted Miocene tholeiite (GC1262; Hoernle *et al.*, 1991; Hoernle & Schmincke, 1993*a*) and the isotopic composition of the Late Miocene rocks were used. The crustal end-members were sample 303905, which has the most radiogenic Sr (0·7052) and highest Sr concentrations (157 ppm) of the igneous crustal samples, and sample 303906, which has among the least radiogenic Pb ($^{206}Pb/^{204}Pb = 18·4$) and the highest Pb concentration (3·6 ppm) of the igneous crustal samples. The mafic post-Miocene volcanic rocks (*mg*-number $\geqslant 62$) generally have less radiogenic Sr but more radiogenic Nd and Pb than the evolved post-Miocene volcanic rocks. In the Pb isotope diagram (b), the alkalic rocks (alkali basalts through trachytes and basanites–melilitites through phonolites) fall below or straddle the NHRL, whereas the Pliocene tholeiites (○) form a vertical trend going towards sediments. An alkali basalt flow, directly beneath the tholeiites, is also shown (●). Data sources are Crisp & Spera (1987), Cousens *et al.* (1990), Hoernle *et al.* (1991, 1995) and Thirlwall *et al.* (1997).

minimum of 30% assimilation of altered igneous crust is required to explain the range in Sr and Pb isotope ratios in the Early Miocene basalts. Such large amounts of assimilation are unlikely based on thermal considerations. In addition, assimilation of local oceanic crust by the Early Miocene basaltic melts cannot explain correlations

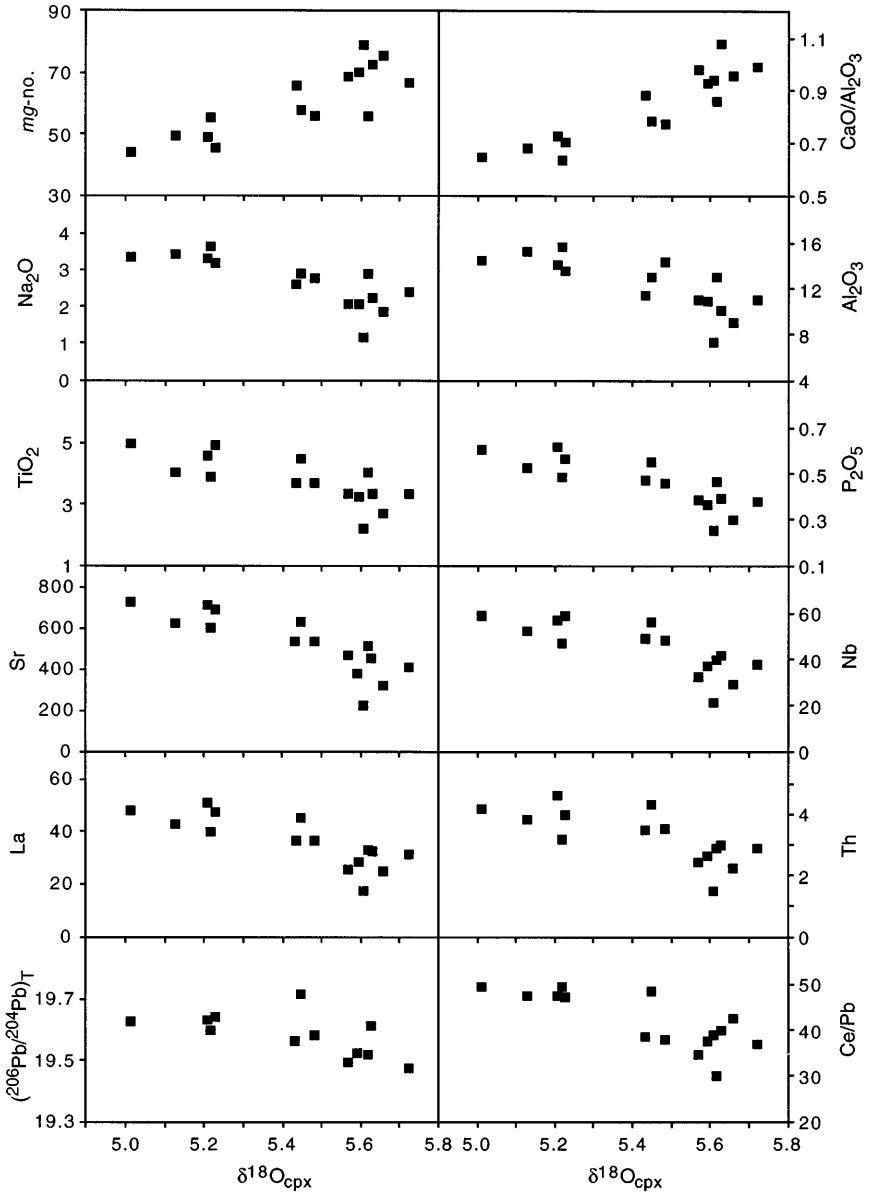

Fig. 10. $\delta^{18}O_{cpx}$ in the Early Miocene shield basalts correlates positively with *mg*-number [i.e. molar Mg/(Mg + 0·8Fe*), where Fe* is total iron] and CaO/Al_2O_3, and negatively with Al_2O_3, Na_2O, TiO_2, P_2O_5, Sr, Nb, La, Th, $^{206}Pb/^{204}Pb$ and Ce/Pb. The three samples showing evidence for sediment assimilation are not plotted. Average $\delta^{18}O_{cpx}$ is plotted when multiple analyses were made on the same sample. Data are from Thirlwall *et al.* (1997).

of $^{206}Pb/^{204}Pb$ with $^{208}Pb/^{204}Pb$ (Fig. 7a) and highly incompatible trace element ratios, such as Ce/Pb, Nd/Pb, Ce/P and Zr/Nb (Fig. 11). In plots of $^{206}Pb/^{204}Pb$ vs $^{208}Pb/^{204}Pb$, Ce/Pb and Nd/Pb, two-component mixing will form linear arrays. Although the Miocene data form linear arrays in these diagrams, the field for the igneous crust beneath Gran Canaria does not fall on extensions of these arrays. Finally, the Early Miocene basalts have higher Ce/P and Zr/Nb ratios than the Late Miocene rocks and the local igneous crust and therefore cannot reflect mixtures between these two components.

As assimilation of igneous oceanic crust appears to be an inadequate explanation for the observed variations in the Miocene volcanic rocks, the low $\delta^{18}O$ ratios and high $^{206}Pb/^{204}Pb$ and Ce/Pb ratios could indicate the presence of recycled igneous oceanic crust in the Canary plume (Hoernle *et al.*, 1991; Marcantonio *et al.*, 1995; Thirlwall *et al.*, 1997). The $\delta^{18}O$ in olivine (4·8–5·5‰) from primitive

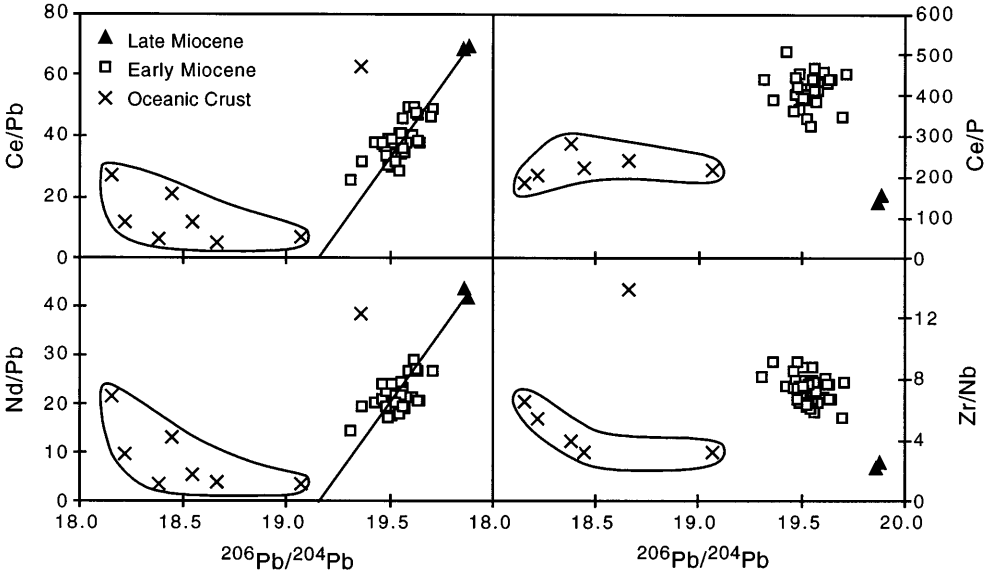

Fig. 11. Assimilation of the igneous ocean crust beneath Gran Canaria cannot explain the correlations of $^{206}Pb/^{204}Pb$ with Ce/Pb, Nd/Pb, Ce/P and Zr/Nb. Data sources: Cousens *et al.* (1990); Hoernle & Schmincke (1993*a*); Thirlwall *et al.* (1997); Schmincke *et al.* (1998).

Pliocene and Quaternary basalts from all of the Canary Islands shows very similar correlations with whole-rock chemistry (Wiechert *et al.*, 1997) to $\delta^{18}O$ in clinopyroxene from the Miocene shield basalts on Gran Canaria. The high incompatible element concentrations in low $\delta^{18}O_{ol}$ samples are compatible with the melting of garnet pyroxenite, which was formerly hydrothermally altered oceanic crust (Wiechert *et al.*, 1997).

Studies of ultramafic massifs and mantle xenoliths show that pyroxenite may make up 2–5% of the upper mantle (Hirschmann & Stolper, 1996). Based in part on the observation that pyroxenite layers in orogenic massifs have significantly more radiogenic Pb isotope ratios than the associated peridotite (Hamelin & Allègre, 1988), Hirschmann & Stolper (1996) proposed that correlations between Pb isotope ratios and incompatible element ratios influenced by garnet in the residuum would provide evidence for garnet pyroxenite in the source. Therefore, the positive correlation between $^{206}Pb/^{204}Pb$ and Zr/Y (Fig. 12) and the more radiogenic Pb and higher Sm/Yb ratios in the Late Miocene than the Early Miocene basalts (Hoernle *et al.*, 1991; Hoernle & Schmincke, 1993*a*; Thirlwall *et al.*, 1997) provide further support for the presence of garnet pyroxenite in the Miocene source. The presence of garnet pyroxenite in the source could also explain the apparent paradox between the relatively shallow depths of melting (40–80 km) estimated from the SiO_2 content (46–50%) of primitive Miocene basalts (after Hirose & Kushiro, 1993) and the rare earth element evidence for garnet in the residuum (Hoernle & Schmincke, 1993*a*). The major element correlations with $\delta^{18}O$ in the Miocene Gran Canaria rocks (Fig. 10) are also qualitatively consistent with melting of pyroxenite, as mantle pyroxenites extend to much lower *mg*-number (as low as 45) and higher Al_2O_3 (as high as 20 wt %) than mantle peridotite (Hirschmann & Stolper, 1996). Finally, the composition of the Late Miocene basalts (Hoernle & Schmincke, 1993*a*) is very similar to the composition of melts derived during experiments on the melting of synthetic pyroxenite at 25 kbar (Hirschmann *et al.*, 1995).

In summary, out of the 75 Miocene basalt samples studied for Sr, Nd, Pb and/or O isotopes (Sun, 1980; Cousens *et al.*, 1990; Hoernle *et al.*, 1991; Thirlwall *et al.*, 1997), only three samples (4% of the total) show clear evidence for $\geqslant 2\%$ crustal assimilation. The isotopic variations in the remaining samples appear to primarily reflect melting of a heterogeneous plume source containing pyroxenite layers within a peridotitic matrix. The general shift towards more radiogenic Pb isotopic composition with decreasing age during the Miocene suggests that the pyroxenite component is preferentially sampled during the late stages of shield volcanism. During the Early Miocene stage of volcanism, Gran Canaria was presumably closer to the hotter center of the plume. A longer melting interval resulted in higher degrees of melting and thus a larger contribution from the peridotite component (higher peridotite/pyroxenite ratio). During the Late Miocene stage, Gran Canaria was further from the plume center. A shorter melting interval resulted in lower degrees of melting and a smaller contribution from the peridotite component (higher pyroxenite/peridotite ratio).

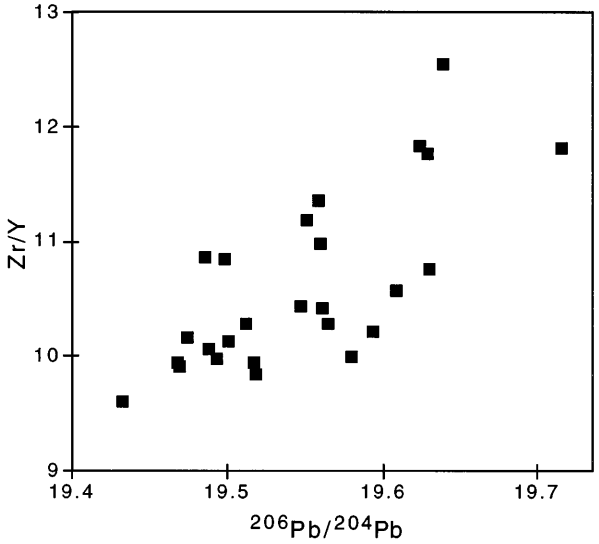

Fig. 12. $^{206}Pb/^{204}Pb$ correlates positively with Zr/Y for the Early Miocene basaltic rocks, suggesting the presence of garnet pyroxenite in the source (Hirschmann & Stolper, 1996). Data sources are the same as in Fig. 11.

The post-Miocene alkalic rocks form arrays in isotope correlation diagrams consistent with two-component mixing (Fig. 9). Mafic volcanic rocks have more radiogenic Pb and Nd and less radiogenic Sr and are believed to reflect the compositions of their asthenospheric sources, whereas the evolved rocks extend to the least radiogenic Pb and Nd but most radiogenic Sr and are interpreted as reflecting lithospheric contamination (Hoernle *et al.*, 1991). The low $^{143}Nd/^{144}Nd$ and $^{207}Pb/^{204}Pb$ isotope ratios in the evolved samples, however, are not consistent with assimilation of either sediments or igneous oceanic crust (Fig. 9).

Two possible candidates for the evolved end-member are ancient ($\geq$2 gy) (a) lower continental crustal material (e.g. granulite) or (b) enriched (EM1-type) subcontinental lithospheric mantle, similar to that sampled by the Smoky Butte lamproites (Fraser *et al.*, 1986). Although it is possible that a block of lower continental crust was incorporated within the Gran Canaria oceanic crust during rifting of Africa from North America, nothing to date has been found within the crust with an appropriate Sr–Nd–Pb isotopic composition. Alternatively, this component may be located within the lithospheric mantle. A study of Os–Sr–Nb–Pb isotopes of <100 000-year-old basalts from the Canary Islands shows that some enriched (EM-type) material is located within the lithospheric mantle beneath at least the eastern Canary Islands (Widom *et al.*, 1998*b*). Additional support for a mantle origin for the enriched component comes from the low $\delta^{18}O_{ol}$ of 5·28‰ (Wiechert *et al.*, in preparation) for basalt sample RNB60, which has relatively unradiogenic Nd (0·51283, Hoernle *et al.*, 1991) and Pb (Table 2b) isotope ratios. Two possible mechanisms for enriching parts of the lithospheric mantle beneath the eastern Canary Islands include metasomatism by earlier melts from the Canary plume (Hoernle & Tilton, 1991) and incorporation of enriched pockets of subcontinental lithospheric mantle during or after rifting to form the Atlantic (Hoernle *et al.*, 1991).

The Pliocene tholeiites form a vertical trend in the uranogenic Pb diagram (Fig. 9b) suggestive of crustal assimilation. The increase in $^{207}Pb/^{204}Pb$ ratio, however, does not correlate with either Sr or Nd isotopes. Considering the high Pb content of some sediments (e.g. 27 ppm was measured in one sediment xenolith, whereas manganese crusts and sulfides typically have Pb concentrations in the 100–1000 ppm range), the difference in $^{207}Pb/^{204}Pb$ could be generated by <2% sediment assimilation (without taking into account the error on the $^{207}Pb/^{204}Pb$ ratio), which would not significantly affect the Sr and Nd isotopic composition of these samples.

The post-Miocene mafic alkaline volcanic rocks, which are interpreted to have isotopic compositions similar to their asthenospheric sources, have less radiogenic Pb and extend to more radiogenic Nd than the Miocene igneous rocks (Fig. 9). Entrainment of depleted (MORB) mantle or recently subducted (within the last 0·5 gy), unaltered oceanic crust by a plume with a composition similar to the Miocene rocks could have generated the post-Miocene source.

In conclusion, based on the data available at present for the crust beneath Gran Canaria, the isotopic composition of the volcanic rocks appears to primarily reflect the composition of their mantle sources rather than crustal assimilation. Considering that the subaerial

portion of Gran Canaria (and most ocean island volcanoes) represents the latest stages of magmatism and <2% of the total volume of the volcano, crustal assimilation may primarily occur during the seamount stage of activity. A well-insulated magma plumbing system is likely to have developed by the time the seamount emerges as an ocean island.

CONCLUSIONS

(1) This study confirms that the samples from Barranco de Balos are from the oceanic crust, which has an age of 178 $\pm$ 17 Ma (determined from Sm–Nd isotope systematics).

(2) Hydrothermal alteration near the ridge axis can increase the $^{238}U/^{204}Pb$ and Ce/Pb ratios to values as high as 107 and 133 respectively, but does not appear to significantly affect Nb/U or $^{232}Th/^{238}U$ ratios.

(3) Seafloor alteration–metamorphism and subsequent radiogenic ingrowth can generate extreme heterogeneity within old ocean crust. The Jurassic crust beneath Gran Canaria has $^{87}Sr/^{86}Sr$ = 0·7029–0·7052, $^{143}Nd/^{144}Nd$ = 0·51295–0·51306, $^{206}Pb/^{204}Pb$ = 18·2–20·8, $^{207}Pb/^{204}Pb$ = 15·59–15·73 and $^{208}Pb/^{204}Pb$ = 38·1–41·3. The range in $^{87}Sr/^{86}Sr$, $^{206}Pb/^{204}Pb$ and $^{208}Pb/^{204}Pb$ is $\geq$50% of that observed in world-wide OIB.

(4) Some regions of altered Jurassic oceanic crust already have trace element characteristics and isotopic compositions similar to end-member HIMU. For example, sample B9117.3 has $^{87}Sr/^{86}Sr$ (0·7029), $^{143}Nd/^{144}Nd$ (0·51295), $^{206}Pb/^{204}Pb$ (20·8) and $^{207}Pb/^{204}Pb$ (15·73) within the ranges reported for St Helena, the Atlantic HIMU-type end-member. Age estimates for generating end-member HIMU compositions (Cameroon Line, St Helena and Mangaia) from Gran Canaria oceanic crust range from 115–223 Ma to 700–1100 Ma.

(5) The Sr, Nd, Pb and O isotopic composition of magmas that formed the subaerial part of Gran Canaria appear to primarily reflect the composition of their mantle sources. The chemical variations in the Miocene or shield cycle of volcanism can best be explained by melting of a heterogeneous plume containing layers of garnet pyroxenite within a peridotite matrix.

ACKNOWLEDGEMENTS

I am indebted to Hans Schmincke for finding the sample locality and encouraging me to work on these samples, and to the UCSC and UCSB isotope groups for allowing me to use their facilities. George Tilton is thanked for analyzing one of the samples. Hans Schmincke, Jim Gill, Liz Widom, Dave Graham and Thor Hansteen helped collect the samples. Thor Hansteen prepared the samples and provided me with important background material needed to complete this study. Insightful discussions with and/or reviews of earlier versions of this manuscript by Uwe Wiechert, Dave Graham, Barry Hanan, Al Hofmann, George Tilton, Thor Hansteen, Colin Devey and Hans Schmincke influenced my interpretations. Formal reviews by Matthew Thirlwall, Mike Garcia, Ian Ridley and Hubert Staudigel were for the most part constructive and helped significantly improve this manuscript. Uwe Wiechert, Else-Ragnhild Neumann and Martin Whitehouse are thanked for the use of their unpublished data. Finally, I am grateful to Dieter Garbe-Schönberg, Susanne Dorn and Folkmar Hauff for carrying out the ICP-MS analyses. Financial support was provided by the National Science Foundation (EAR-9105113).

REFERENCES

Barling, J. & Goldstein, S. L. (1990). Extreme isotopic variations in Heard Island lavas and the nature of mantle reservoirs. *Nature* **348,** 59–62.

Barling, J., Goldstein, S. L. & Nicholls, I. A. (1994). Geochemistry of Heard Island (southern Indian Ocean): characterization of an enriched mantle component and implications for enrichment of the sub-Indian ocean mantle. *Journal of Petrology* **35,** 1017–1053.

Ben Othman, D., White, W. M. & Patchett, J. (1989). The geochemistry of marine sediments, island arc magma genesis, and crust–mantle recycling. *Earth and Planetary Science Letters* **94,** 1–21.

Chaffey, D. J., Cliff, R. A. & Wilson, B. M. (1989). Characterization of the St Helena magma source. In: Saunders, A. D.& Norry, M. J. (eds) *Magmatism in the Ocean Basins. Geological Society, London, Special Publication* **42,** 257–276.

Chase, C. (1981). Oceanic island Pb: two-stage histories and mantle evolution. *Earth and Planetary Science Letters* **52,** 277–284.

Cousens, B. L., Spera, F. J. & Tilton, G. R. (1990). Isotopic patterns in silicic ignimbrites and lava flows of the Mogan and lower Fataga Formations, Gran Canaria, Canary Islands: temporal changes in mantle source composition. *Earth and Planetary Science Letters* **96,** 319–335.

Cousens, B. L., Spera, F. J. & Dobson, P. F. (1993). Post-eruptive alteration of silicic ignimbrites and lavas, Gran Canaria, Canary Islands: strontium, neodymium, lead, and oxygen isotopic evidence. *Geochimica et Cosmochimica Acta* **57,** 631–640.

Crisp, J. A. & Spera, F. J. (1987). Pyroclastic flows and lavas of the Mogan and Fataga formations, Tejeda Volcano, Gran Canaria, Canary Islands: mineral chemistry, intensive parameters, and magma chamber evolution. *Contributions to Mineralogy and Petrology* **96,** 503–518.

Davies, G. R., Norry, M. J., Gerlach, D. C. & Cliff, R. A. (1989). A combined chemical and Pb–Sr–Nd isotope study of the Azores and Cape Verde hot-spots: the geodynamic implications. In: Saunders, A. D. & Norry, M. J. (eds) *Magmatism in the Ocean Basins. Geological Society, London, Special Publication* **42,** 231–255.

Dosso, L., Hanan, B., Bougault, H., Schilling, J.-G. & Joron, J.-L. (1991). Sr–Nd–Pb geochemical morphology between 10° and 17°N on the Mid-Atlantic Ridge: a new MORB isotope signature. *Earth and Planetary Science Letters* **106,** 29–43.

Eiler, J. M., Farley, K. A., Valley, J. W., Hofmann, A. W. & Stolper, E. M. (1996*a*). Oxygen isotope constraints on the sources of Hawaiian volcanism. *Earth and Planetary Science Letters* **144,** 453–468.

Eiler, J. M., Valley, J. W. & Stolper, E. M. (1996*b*). Oxygen isotope ratios in olivine from the Hawaii Scientific Drilling Project. *Journal of Geophysical Research* **101,** 11807–11813.

Elliot, T. R., Hawkesworth, C. J. & Grönvold, K. (1991). Dynamic melting of the Iceland plume. *Nature* **351,** 201–206.

Faure, G. (1986). *Principles of Isotope Geology*. New York: John Wiley.

Fraser, K. J., Hawkesworth, C. J., Erlank, A. J., Mitchell, R. H. & Scott-Smith, B. H. (1986). Sr, Nd, and Pb isotope and minor element geochemistry of lamproites and kimberlites. *Earth and Planetary Science Letters* **76,** 57–70.

Freundt, A. & Schmincke, H.-U. (1995). Petrogenesis of rhyolite–trachyte–basalt composite ignimbrite P1, Gran Canaria, Canary Islands. *Journal of Geophysical Research* **100,** 455–474.

Furman, T., Frey, F. A. & Kye-Hum Park (1991). Chemical constraints on the petrogenesis of mildly alkaline lavas from Vestmanmaeyjar, Iceland: the Eldfell (1973) and Surtsey (1963–1967) eruptions. *Contributions to Mineralogy and Petrology* **109,** 19–37.

Garbe-Schönberg, C.-D. (1993). Simultaneous determination of thirty-seven trace elements in twenty-eight international rock standards by ICP-MS. *Geostandards Newsletters* **17,** 81–97.

Halliday, A. N., Dickin, A. P., Fallick, A. E. & Fitton, J. G. (1988). Mantle dynamics: a Nd, Sr, Pb and O isotopic study of the Cameroon Line volcanic chain. *Journal of Petrology* **29,** 181–211.

Halliday, A. N., Davidson, J. P., Holden, P., DeWolf, C., Lee, D.-C. & Fitton, J. G. (1990). Trace-element fractionation in plumes and the origin of HIMU mantle beneath the Cameroon line. *Nature* **347,** 523–528.

Hamelin, B. & Allègre, C. J. (1988). Lead isotope study of orogenic lherzolite massifs. *Earth and Planetary Science Letters* **91,** 117–131.

Hanan, B. B. & Graham, D. W. (1996). Lead and helium isotope evidence from oceanic basalts for a common deep source of mantle plumes. *Science* **272,** 991–995.

Hart, S. R. (1984). A large-scale isotope anomaly in the Southern Hemisphere mantle. *Nature* **309,** 753–757.

Hart, S. R. & Staudigel, H. (1989). Isotopic characterization and identification of recycled components. In: Hart, S. R. & Gülen, L. (eds) *Crust/Mantle Recycling at Convergence Zones. NATO ASI Series C 258*. Dordrecht: Kluwer Academic, pp. 15–28.

Hawkesworth, C. J., Norry, M. J., Roddick, J. C. & Vollmer, R. (1979). $^{143}Nd/^{144}Nd$ and $^{87}Sr/^{86}Sr$ ratios from the Azores and their significance in LIL-element enriched mantle. *Nature* **280,** 28–31.

Hirose, K. & Kushiro, I. (1993). Partial melting of dry peridotites at high pressures: determination of compositions of melts segregated from peridotite using aggregates of diamond. *Earth and Planetary Science Letters* **114,** 477–489.

Hirschmann, M. M. & Stolper, E. M. (1996). A possible role for garnet pyroxenite in the origin of the 'garnet signature' in MORB. *Contributions to Mineralogy and Petrology* **124,** 185–208.

Hirschmann, M. M., Baker, M. B. & Stolper, E. M. (1995). Partial melting of mantle pyroxenite (abstract). *EOS Transactions, American Geophysical Union* **76,** F696.

Hoernle, K. & Schmincke, H.-U. (1993*a*). The petrology of the tholeiites through melilite nephelinites on Gran Canaria, Canary Islands: crystal fractionation, accumulation, and depths of melting. *Journal of Petrology* **34,** 573–597.

Hoernle, K. & Schmincke, H.-U. (1993*b*). The role of partial melting in the 15-Ma geochemical evolution of Gran Canaria: a blob model for the Canary hotspot. *Journal of Petrology* **34,** 599–626.

Hoernle, K. A. & Tilton, G. R. (1991). Sr–Nd–Pb isotope data for Fuerteventura (Canary Islands) basal complex and subaerial volcanics: applications to magma genesis and evolution. *Schweizerische Mineralogische und Petrographische Mitteilungen* **71,** 3–18.

Hoernle, K., Tilton, G. & Schmincke, H.-U. (1991). Sr–Nd–Pb isotopic evolution of Gran Canaria: evidence for shallow enriched mantle beneath the Canary Islands. *Earth and Planetary Science Letters* **106,** 44–63.

Hoernle, K., Zhang, Y.-S. & Graham, D. (1995). Seismic and geochemical evidence for large-scale mantle upwelling beneath the eastern Atlantic and western and central Europe. *Nature* **374,** 34–39.

Hofmann, A. W. (1988). Chemical differentiation of the earth: the relationship between mantle, continental crust, and oceanic crust. *Earth and Planetary Science Letters* **90,** 297–314.

Hofmann, A. W. & White, W. H. (1982). Mantle plumes from ancient oceanic crust. *Earth and Planetary Science Letters* **57,** 421–436.

Hofmann, A. W., Jochum, K. P., Seufert, M. & White, W. M. (1986). Nb and Pb in oceanic basalts: new constraints on mantle evolution. *Earth and Planetary Science Letters* **79,** 33–45.

Ito, E., White, W. M. & Göpel, C. (1987). The O, Sr, Nd and Pb isotope geochemistry of MORB. *Chemical Geology* **62,** 157–176.

Klitgord, K. D. & Schouten, H. (1986). Plate kinematics of the Central Atlantic. In: Vogt, P. R. & Tucholke, B. E. (eds) *The Geology of North America, Vol. M, The Western North Atlantic Region*. Boulder, CO: Geological Society of America, pp. 351–378.

Kogiso, T., Yoshiyuki, T. & Nakano, S. (1997). Trace element transport during dehydration processes in the subducted oceanic crust: 1. Experiments and implications for the origin of ocean island basalts. *Earth and Planetary Science Letters* **148,** 193–205.

Marcantonio, F., Zindler, A., Elliot, T. & Staudigel, H. (1995). Os isotope systematics of La Palma, Canary Islands: evidence for recycled crust in the mantle source of HIMU ocean islands. *Earth and Planetary Science Letters* **133,** 397–410.

Mattey, D., Lowry, D. & Macpherson, C. (1994). Oxygen isotope composition of mantle peridotite. *Earth and Planetary Science Letters* **128,** 231–241.

Nakamura, Y. & Tatsumoto, M. (1988). Pb, Nd, and Sr isotopic evidence for a multicomponent source for rocks of Cook–Austral Islands and heterogeneities of mantle plumes. *Geochimica et Cosmochimica Acta* **52,** 2909–2924.

Nicholson, H., Condomines, M., Fitton, J., Fallick, A., Grönvold, K. & Rogers, G. (1991). Geochemical and isotopic evidence for crustal assimilation beneath Krafla, Iceland. *Journal of Petrology* **32,** 1005–1020.

Richardson, S. H., Erlank, A. J., Duncan, A. R. & Reid, D. L. (1982). Correlated Nd, Sr and Pb isotope variation in Walvis Ridge basalts and implications for the evolution of their mantle source. *Earth and Planetary Science Letters* **59,** 327–342.

Roeser, H. A. (1982). Magnetic anomalies in the magnetic quiet zone off Morocco. In: von Rad, U., Hinz, K., Sarnthein, M. & Seibold, E. (eds) *Geology of the Northwest African Continental Margin*. Berlin: Springer-Verlag, pp. 60–68.

Roest, W. R., Dañobeitia, J. J., Verhoef, J. & Collette, B. J. (1992). Magnetic anomalies in the Canary Basin and the Mesozoic evolution of the Central North Atlantic. *Marine Geophysical Research* **14,** 1–24.

Schilling, J.-G., Hanan, B. B., McCully, B. & Kingsley, R. H. (1994). Influence of the Sierra Leone mantle plume on the equatorial Mid-Atlantic Ridge: a Nd–Sr–Pb isotopic study. *Journal of Geophysical Research* **99,** 12005–12028.

Schmincke, H.-U. (1982). Volcanic and chemical evolution of the Canary Islands. In: von Rad, U., Hinz, K., Sarnthein, M. & Seibold, E. (eds) *Geology of the Northwest African Margin*. New York: Springer-Verlag, pp. 273–306.

Schmincke, H. U., Freundt, A., Rihm, R., Sumita, M., Krastel, S. & Hoernle, K. (1997). Vulkaninseln als ozeanische Geosysteme. *Geowissenschaften* **15**(9), 301–305.

Schmincke, H.-U., Klügel, A., Hoernle, K., Hansteen, T. H., & van den Bogaard, P. (1998). Samples from the Jurassic ocean crust beneath Gran Canaria, La Palma and Lanzarote (Canary Islands). *Earth and Planetary Science Letters*, (submitted).

Silver, P. G., Carlson, R. W. & Olson, P. (1988). Deep slabs, geochemical heterogeneity, and the large-scale structure of mantle convection: investigation of an enduring paradox. *Annual Review of Earth and Planetary Sciences* **16,** 477–541.

Staudigel, H., Hart, S. R. & Richardson, S. H. (1981). Alteration of the oceanic crust: processes and timing. *Earth and Planetary Science Letters* **52,** 311–327.

Staudigel, H., Davies, G. R., Hart, S. R., Marchant, K. M. & Smith, B. M. (1995). Large scale isotopic Sr, Nd and O isotopic anatomy of altered oceanic crust: DSDP/ODP sites 417/418. *Earth and Planetary Science Letters* **130,** 169–185.

Storey, M., Saunders, A. D., Tarney, J., Leat, P., Thirlwall, M. F., Thompson, R. N., Menzies, M. A. & Marriner, G. F. (1988). Geochemical evidence for plume–mantle interactions beneath Kerguelen and Heard Islands, Indian Ocean. *Nature* **336,** 371–374.

Sun, S. S. (1980). Lead isotopic study of young volcanic rocks from mid-ocean ridges, ocean islands and island arcs. *Philosophical Transactions of the Royal Society of London, Series A* **297,** 409–445.

Sun, S.-S. & McDonough, W. F. (1989). Chemical and isotopic systematics of oceanic basalts: implications for mantle composition and processes. In: Saunders, A. D. & Norry, M. J. (eds) *Magmatism in the Ocean Basins. Geological Society, London, Special Publication* **42,** 313–345.

Thirlwall, M. F. (1997). Pb isotopic and elemental evidence for OIB derivation from young HIMU mantle. *Chemical Geology* **139,** 51–74.

Thirlwall, M. F., Jenkins, C., Vroon, P. Z. & Mattey, D. P. (1997). Crustal interaction during construction of ocean islands: Pb–Sr–Nd–O isotope geochemistry of the shield basalts of Gran Canaria, Canary Islands. *Chemical Geology* **135,** 233–262.

Vance, D. J., Stone, J. O. H. & O'Nions, R. K. (1989). He, Sr and Nd isotopes in xenoliths from Hawaii and other oceanic islands. *Earth and Planetary Science Letters* **96,** 147–160.

Vidal, P. H., Chauvel, C. & Brousse, R. (1984). Large mantle heterogeneity beneath French Polynesia. *Nature* **307,** 536–538.

White, R. S., McKenzie, D. & O'Nions, R. K. (1992). Oceanic crustal thickness from seismic and rare earth element inversions. *Journal of Geophysical Research* **97,** 19683–19715.

White, W. M. (1993). $^{238}U/^{204}Pb$ in MORB and open system evolution of the depleted mantle. *Earth and Planetary Science Letters* **115,** 211–226.

White, W. M., Tapia, M. D. M. & Schilling, J.-G. (1979). The petrology and geochemistry of the Azores Islands. *Contributions to Mineralogy and Petrology* **69,** 201–213.

Widom, E. & Shirey, S. B. (1996). Os isotope systematics in the Azores: implications for mantle plume sources. *Earth and Planetary Science Letters* **142,** 451–465.

Widom, E., Carlson, R. W., Gill, J. B. & Schmincke, H.-U. (1998*a*). The Th–Sr–Nd–Pb isotope and trace element evidence for the origin of the São Miguel, Azores, enriched mantle source. *Chemical Geology* (submitted).

Widom, E., Hoernle, K. A., Shirey, S. B. & Schmincke, H.-U. (1998*b*). Os isotope systematics in the Canary Islands and Madeira: lithospheric contamination and mantle plume signatures. *Journal of Petrology* (in press).

Wiechert, U., Hoernle, K. & Graham, D. (1997). Oxygen isotope evidence for high temperature altered oceanic crust in the Canary Plume (abstract). *EOS Transactions, American Geophysical Union* **78,** F825–826.

Woodhead, J. D. & McCulloch, M. T. (1989). Ancient seafloor signals in Pitcairn Island lavas and evidence for large amplitude, small length-scale mantle heterogeneities. *Earth and Planetary Science Letters* **94,** 257–273.

Wright, E. & White, W. M. (1987). The origin of Samoa, new evidence from Sr, Nd, and Pb isotopes. *Earth and Planetary Science Letters* **81,** 151–162.

Ye, S., Rihm, R., Dañobeitia, J. J., Canales, J. P. & Gallart, J. (1998). A crustal transect through the northern and northeastern part of the volcanic edifice of Gran Canaria. *Journal of Geodynamics* (in press).

Zindler, A. & Hart, S. (1986). Chemical geodynamics. *Annual Review of Earth and Planetary Sciences* **14,** 493–571.